Loan copy

NATIONAL ADVISORY COMMITTEE FOR AERONAUTICS

TECHNICAL NOTE

No. 1090

THE SHEARING RIGIDITY OF CURVED PANELS UNDER COMPRESSION

By N. J. Hoff and Bruno A. Boley
Polytechnic Institute of Brooklyn



Washington
August 1946

NATIONAL ADVISORY COMMITTEE FOR AERONAUTICS

TECHNICAL NOTE NO. 1090

THE SHEARING RIGIDITY OF CURVED PANELS UNDER COMPRESSION

By N. J. Hoff and Bruno A. Boley

SUMMARY

Experiments were carried out at Polytechnic Institute of Brooklyn Aeronautical Laboratories in order to determine the shearing rigidity of curved panels under compression, particularly in that region of loading where the panels are in a buckled state. For the preliminary tests four, and for the final test series eight, circular cylinders were built of aluminum alloy sheet. The cylinders were reinforced with a number of stringers and rings. The tests were made by measuring the angle of twist of the cylinder caused by known amounts of torque while the cylinder was subjected to uniform axial compression.

It was found that the shearing rigidity decreases with increasing compression, and the lowest value measured was about one-tenth of the original value. The results of the investigation are presented graphically and by means of an approximate empirical formula. Use is made of the nondimensional parameters ϵ/ϵ_{cr} and r/d, where ϵ is the axial compressive strain in the stringers, ϵ_{cr} its value when the panel buckles, r the radius of the cylinder, and d the stringer spacing measured along the circumference. In the experiments the value of ϵ/ϵ_{cr} varied approximately from 0 to 15, that of r/d from 1 to 2.5.

INTRODUCTION

While two other research projects were being carried out at Polytechnic Institute of Brooklyn Aeronautical Laboratories it was found that it would be desirable to investigate the variation with increasing compressive stress of the shearing

rigidity of curved panels which are in a buckled state because of the compression. One of these projects dealt with the calculation of the stress distribution in monocoque cylinders (reference 1). Because of the lack of data on the shearing rigidity the calculations had to be restricted to cases of loading in which the panels were in a non-buckled state and thus a comparison with test results (reference 2) was possible only for low load conditions.

The other research project was a theoretical investigation of the general instability of monocoque cylinders in pure bending. In the absence of experimental data the theory of the inward bulge type general instability was developed in reference 3 on the basis of an assumed variation of the apparent shearing rigidity of the panels along the circumference of the monocoque cylinder. It is desirable to replace this assumption by data derived from experiment and to extend the applicability of the numerical procedures mentioned to cases of loading in which some of or all the panels are in a buckled state. The effective shear modulus values should also be useful in other calculations of the stress distribution, for instance, in shear lag analyses by Paul Kuhn's method (references 4 and 5).

The experimental investigation described in this report was undertaken in order to furnish these data.

It is believed that the simplest method by which uniformly distributed shearing stresses can be applied to thin sheet consists in twisting a cylinder made of thin sheet. If the cylinder is circular, and the stringers are attached to its circumference at uniform intervals, plane sections before torsion remain plane during the loading and no warping moments are introduced by the end fixtures.

In the preliminary experiments four and in the final series eight reinforced monocoque cylinders were tested by applying first a uniformly distributed axial compressive force and then measuring the angle of twist of the cylinder under a simultaneously applied torque. The effective shear modulus G_{eff} was defined as the value that makes Bredt's formula valid even though the panels are in a buckled state because of the compression.

In reference 6 it was suggested that the apparent or effective shearing rigidity would depend on the ratio of compressive stress to critical compressive stress and on the

difference between the chord length and the arc length of the non-buckled panel. The two parameters ϵ/ϵ_{cr} and r/d used in this report represent these quantities in a nondimensional form.

The preliminary work was carried out by Albert J. Cullen, and the final investigation by the junior author. The former was assisted by Edgar B. Beck and the latter by Joseph D. Windischmann. The project was under the direction of the senior author. It was sponsored by, and conducted with financial assistance from, the National Advisory Committee for Aeronautics.

LIST OF SYMBOLS

a	side length of a square section
A	area enclosed by the circumference of the cylinder
C	geometric factor in torsional rigidity GC
d	width of panel measured along the circumference
D	diameter of cylinder
E	Young's modulus
F_{cy}	yield-point stress
G	shear modulus
G_o	shear modulus of cylinder at zero compressive load
G_{eff}	effective shear modulus
I	moment of inertia
I_p	polar moment of inertia
k	nondimensional coefficient used in the formula for the buckling strain of a flat panel
K	$= LS/4A^2t$
L	length of cylinder

n	number of stringers
N	$= 0.0275(n + 1)$
P	axial compressive force
Q	force
r	radius of cylinder
S	circumference of cylinder
t	thickness of sheet covering
T	torque
$2w$	effective width of flat panel
$2w'$	effective width of curved panel
ϵ	normal strain
ϵ_{cr}	buckling strain of panel
ϵ_{curved}	buckling strain of non-reinforced circular cylinder under uniform axial compression
ϵ_{flat}	buckling strain of flat panel under uniform compression
ϵ_{str}	axial compressive strain in the stringers
φ	angle of twist
φ_{mean}	harmonic mean of angles of twist measured in the upper and lower halves of the cylinder

Subscripts

L	lower
U	upper

DESCRIPTION OF TESTS

Final Series

One of the test cylinders of the final series is shown in figure 1. It has a diameter of 16 inches and is made of 0.012-inch thick 24S-T Alclad sheet. Its reinforcement consists of 4 rings and 12 equidistant stringers made of 3/8- by 3/8-inch square section 24S-T aluminum alloy bars. For the convenience of manufacture the rings are arranged outside and the stringers inside the cylindrical sheet to which they are attached by 1/8-inch diameter A17S-T aluminum alloy round-head rivets.

The characteristics of the various test specimens are listed in table 1. The cylinders of the final series were numbered from 26 to 33. The number of stringers varied from 6 to 16. The ring spacing was 4.5 inches except in cylinder 32 where it was 2.57 inches. In cylinder 31 the rivets attaching the rings to the sheet were omitted and in cylinder 33 they were replaced by screws. The sheet of cylinder 33 was of spring temper brass of the following nominal composition: 72 percent copper and 28 percent zinc. Its thickness was 0.0055 inch.

Two steel one-piece end rings and one steel two-piece middle ring served the purpose of introducing and distributing the external loads. The stringers were attached to the rings by grip fittings of the type described in reference 2. In addition, either 12 or 16 grip fittings of a different kind were used to attach the sheet to each ring, and the inside of the rings was knurled in order to prevent slippage. Details of the attachment are shown in figure 2.

The compressive load was applied by means of a 200,000-pound lever type Riehle Bros. Universal testing machine (fig. 3). Between testing machine and end ring a hard rubber ring and a steel plate, each 1/2 inch thick, were inserted. The uniformity of the stress distribution was checked by measuring the strain in both the upper and the lower half of each cylinder in all the stringers, and in addition in the sheet of two cylinders. The measurements were made by means of metalectric strain gages. The accuracy of the load measurement is better than ± 15 pounds on the Riehle machine; while the maximum error in the strain measurements is about $\pm 1 \times 10^{-5}$.

The torque was applied by means of six links attached at one end to the steel rings, and at the other end to a loading frame which rests on ball bearings as shown in the drawing of figure 4. Details of the torque loading device a are also visible in figures 2 and 3. In the original setup the torque was applied by tightening the nuts at the ends of the middle links. On one middle link the nut was arranged inside the frame so that tightening it caused a compressive force in the link. (See fig. 3.) On the other middle link the nut was outside the frame. Consequently, tightening it caused a tensile force in the link. The forces in the links were measured by metalectric strain gages. When cylinder 26 was tested, strain gages were cemented only to the tension links - that is, to the tension middle link, and to the upper and lower links on the side where the middle link was in compression.

In all the other tests the strain was measured in all the links. From cylinder 30 on, threads and nuts were provided on all the six links in order to insure a more accurate load application. The load links were calibrated on a 30,000-pound lever type Riehle Bros. Universal testing machine. The accuracy of the individual load link readings in the final arrangement was as follows:

Link	(lb)
1	±11
2	±8
3	±12
4	±8.5
5	±18
6	±8

The relative rotation of middle and end rings was measured by Ames dial gages having 1/1000-inch subdivisions. They were attached to the middle ring and their plungers rested on aluminum alloy brackets fastened to the end rings. The accuracy of the measurement of the angle of twist was about ±0.00002 radian.

The testing procedure was as follows: The cylinder was rigged up in the testing machine. The nuts on the load links were tightened and load link readings were made. The nuts were adjusted on the load links until an application of torque was obtained which was considered sufficiently uniform and free of bending. The angle of twise was recorded. The

forces in the load links were then increased in five stages and the procedure of adjusting and reading was repeated at each stage. The angle of twist was plotted against the torque.

The torque was removed and compression applied by lowering the loading head of the testing machine. The strain was measured in all the stringers in both the upper and the lower bands. The compressive strain was adjusted by shimming until a sufficiently uniform strain distribution was obtained. Torque was applied and the angle of twist measured as described in the no-compressive-load case. The stringer strain readings were repeated when the maximum torque was acting upon the cylinder.

With each cylinder the angle of twist versus torque curve was established for from 6 to 12 compressive loads. A complete test took from 2 to 3 days. With a few cylinders the uniformity of the distribution of compressive strain deteriorated considerably in the course of the test. These cylinders were re-shimmed at a low load.

The strains in the sheet were masured in cylinders 27 and 29 by means of pairs of metalectric strain rosettes cemented back to back on opposite sides of the sheet.

Preliminary Tests

Torsion tests were also carried out with cylinders 7, 8, and 10 of the series used for the general instability tests of reference 7. These cylinders had a diameter of 20 inches. Cylinders 7 and 8 were of 0.020-inch thick 24S-T aluminum alloy sheet and cylinder 10 was of 0.012-inch thick Alclad sheet.

The cylinders were fastened to the bending test rig described in detail in reference 7, and the compressive force was applied by tightening the nut on the compressive load bar.

The application of the torque is shown in the sketch of figure 5 and the photograph of figure 6. In the former, A is an interlinked pair of frames between the two units of which a mechanical jack is inserted. When the jack is turned, the movable unit is forced downward and exerts a downward pull upon lever B-B to the midpoint of which it is attached by a pin. One end of lever B-B is linked to one end of lever C-C, while the other ends of the levers are

connected by cable D passing over sheave E. The sheave can rotate around a pin attached to bent F, while lever C-C forms part of loading head G which is rigidly connected to the monocoque test cylinder. The leverage is so constructed that the downward pull at one end of lever C-C is equal to the upward pull at the other end when the jack is cranked. The forces are measured by means of metalectric strain gages cemented to the calibrated load links H. Consequently, a pure torque can be transmitted to the test specimen, and it can be measured accurately. The weight of the loading head with its attachments is balanced by counterweight J.

The angle of twist was measured by means of two Ames dial gages graduated 0.001 inch which were rigidly attached to the load end of the monocoque test cylinder. The Ames gages were 40 inches apart and were arranged symmetrically to the center of the cylinder. Their plungers bore against rigid aluminum alloy bars extending from the fixed end of the monocoque.

Before the cylinders were tested to destruction in the general instability experiments described in reference 7, they were subjected to different compressive loads. At each stage of compression the strain distribution around the circumference was determined. Increasing amounts of torque were then applied to the cylinder and the corresponding angles of twist were recorded. With cylinders 7 and 8 torsion tests were carried out at 3, with cylinder 10 at 6 different values of the compressive load.

Because of limitations of the compression loading device in these preliminary tests, the greatest compressive load applied was only about five times that under which the sheet covering buckled. A new test rig was developed, therefore, and used in testing cylinder 15. This cylinder was very similar to the cylinders of the final series, but the rectangular cross section of its reinforcing rings was 1/8 by 3/8 inch. Compression was applied to the cylinder in the 200,000-pound Riehle Bros. testing machine and the torque was transmitted to the middle ring by means of weights, levers, sheaves, and cables. (See fig. 7.) This test arrangement was abandoned for the test rig described in connection with the final series because it had the following drawbacks: (1) The reactions of the applied torque had to be resisted by the Riehle testing machine. It was not considered permissible to load the testing machine in such a manner when it turned out that the desirable amount of torque was greater than

anticipated. (2) The loading head underwent a rotation because of the torque transmitted to it. Consequently, the lower half of the cylinder carried considerably more torque than the upper half. (3) The application of the weights was inconvenient. (4) The force measurement was not sufficiently reliable.

DISCUSSION OF RESULTS

Uniformity of Compressive Strain

Typical compressive strain distribution curves are shown in figures 8 and 9. In the former are plotted the strains measured in the six stringers and in the middle of the panels of band B of cylinder 29. It may be seen that under a compressive load of 5100 pounds the strain in the sheet is practically the same as that in the stringers. Under a compressive load P = 10,025 pounds the strain in the sheet is slightly less than that in the stringers; while under P = 15,000 pounds the strain in the sheet is little higher than its value under 10,025 pounds. From 15,000 pounds on, the strain in the sheet decreases slightly and the increase in the compressive load is entirely taken by the stringers. Because of the small deviations in the values it was not practicable to plot the sheet strain at loads higher than 15,000 pounds.

While the uniformity of the strain distribution is better than average on figure 8, it is worse than average on figure 9. The latter shows the values obtained with cylinder 33.

The variation of average strain in stringers and sheet with compressive load is presented in figure 10. A theoretical curve is also shown which was calculated from the formulas:

$$2w' = 2w + (\epsilon_{curved}/\epsilon_{str})(d - 2w) \qquad (1)$$

$$2w = [\epsilon_{flat}/(\epsilon_{str} - \epsilon_{curved})]^{1/3}d \qquad (2)$$

where

$2w'$ effective width of a curved panel

$2w$ effective width of a flat panel of equal width

ϵ_{str} strain in the stringer

ϵ_{flat} buckling strain of the flat panel of equal width

ϵ_{curved} buckling strain of a cylinder of equal curvature

d developed width of the curved panel

Equations 1 and 2 are identical with two equations given by Ebner in reference 8, page 26, except for the symbols used. The buckling strain of the flat panel was determined from the equation

$$\epsilon_{flat} = k(t/d)^2 \qquad (3)$$

where t is the thickness of the sheet, and the value of the nondimensional coefficient k was taken from the literature on the basis of considerations given in the next article. In the case of figure 10 (cylinder 29) k was taken as 11.3, while ϵ_{curved} was calculated from the experimental critical strain of 3.3×10^{-4} by means of equation (4). The variation of Young's modulus with compressive strain was taken from reference 9. The agreement between the theoretical and the experimental curves is good.

Buckling of the Panels

Generally, buckling did not occur at the same time in all the panels of the cylinder. In table 2 the buckling strain corresponds to that state of loading in which a great number of the panels passed from the non-buckled state into the buckled state.

The theoretical buckling strain was calculated from Redshaw's formula:

$$\epsilon_{cr} = (\epsilon_{flat}/2) + \sqrt{(\epsilon_{flat}/2)^2 + (\epsilon_{curved})^2} \qquad (4)$$

In this equation the value of ϵ_{flat} was determined from

equation (3). The value of k was taken as the arithmetic mean of the values corresponding to four simply supported edges (p. 309 of reference 10) and four rigidly clamped edges (p. 323 of reference 10). The buckling strain ϵ_{curved} of the circular cylinder of equal radius was computed from Donnell's formula:

$$\epsilon_{curved} = 0.6\,(t/r)\,\frac{1 - 1.7 \times 10^{-7}\,(r/t)^2}{1 + 0.004\,(E/F_{cy})} \qquad (5)$$

It may be seen from table 2 that the theoretical buckling strain is consistently higher than the experimental buckling strain. It is believed that the discrepancy is due to the deviation of the actual shape of the cylinder before loading from the true cylindrical shape. It was observed that because of initial stresses set up during the manufacturing process the panels showed a tendency to pull flat at some distance from the reinforcing rings. In three cylinders the flattening was measured by means of a Geneva Lens Measure. The results of the measurements for a typical panel are shown in figure 11.

Distribution of Shear Strain

The shear strain distribution was determined from the metalectric equilateral strain rosette readings made with cylinders 27 and 29. Figure 12 presents the distribution in cylinder 29 when there is no compressive load. When the compressive load is high enough to cause the panels to buckle, the variation of the strain within the area covered by the rosette makes the readings unreliable.

Calculation of the Effective Shear Modulus

The shear modulus was calculated from the measured values of torque and angle of twist by Bredt's formula:

$$\varphi = (LST)/(4A^2Gt) \qquad (6)$$

where

φ angle of twist

L length of the cylinder

S length of the circumference of the cylinder

A area enclosed by the median line of its wall

G shear modulus

t wall thickness

If the subscript U is used to denote the upper half of the test specimen, the shear modulus becomes on the basis of the test results obtained with the upper half

$$G_U = K(T_U/\varphi_U) \tag{7}$$

where

$$K = (LS)/(4A^2t) \tag{8}$$

In a similar manner the lower half of the test cylinder yields

$$G_L = K(T_L/\varphi_L) \tag{9}$$

The average of the two values of the shear modulus is

$$G_{eff} = (1/2)(G_U + G_L) = (K/2)[(T_U/\varphi_U) + (T_L/\varphi_L)]$$

Since in the tests the difference between T_U and T_L was of the same order of magnitude as the accuracy of the load link measurements, the value of G_{eff} was calculated on the assumption that $T_U = T_L = (T/2)$. In this case

$$G_{eff} = (K/4)T[(1/\varphi_U) + (1/\varphi_L)] \tag{10}$$

where T is the total applied torque.

The applied torque was calculated from the readings of the middle links (links 2 and 5) and was plotted against the average angle of twist φ_{mean} defined as

$$\varphi_{mean} = 1/[(1/\varphi_U) + (1/\varphi_L)] \qquad (11)$$

Figure 13 is a typical example of such a plot. The slope of the straight line multiplied by $K/4$ yields the shear modulus in accordance with equation (10). Whenever the experimental points did not fall on a straight line, the best fitting straight line was calculated by the method of moments presented in reference 11.

The appendix shows that the torsional and bending rigidities of the individual stringers, as well as the rigid fixation of their ends to the end rings, contribute little to the torsional rigidity of the entire cylinder. Consequently, it is permissible to calculate G_{eff} according to the procedure outlined above in which the torsional rigidity of the stringers is neglected. Moreover, it was established experimentally that deviations in the distribution of forces in the load links from the required pattern, which result in the application of bending moments simultaneously with the torque, have a negligible effect upon the angle of twist.

The Shear Rigidity versus Compressive Strain Curves

For each cylinder tested the values of G_{eff} were plotted against the compressive strain. Figures 14 to 21 present these curves for the cylinders of the final test series. The curves obtained in the first three preliminary tests (cylinders 7, 8, and 10) are shown in figure 22, while the curve corresponding to the fourth preliminary test (cylinder 15) is presented in figure 23.

The scatter of the experimental points about the smooth curves is attributed to incidental details of the buckled shape of the panels.

Nondimensional Shear Rigidity Curves

In figure 24 the ratio of G_{eff} to 3.9×10^6 psi is plotted against the ratio of the compressive strain to the buckling strain of the panels for each of the cylinders of the final series. The buckling strain used in plotting these curves was the experimental critical strain listed in table 2. The following observations may be made in connection with figure 24:

1. The shear modulus ratio decreases with increasing compressive strain ratio and seems to approach a horizontal asymptote.

2. In the region $0 < \epsilon / \epsilon_{cr} < 3$ no systematic variation of G_{eff}/G_o can be observed with the number of stringers. It is noted that investigations of the Aluminum Company of America showed random variations of Young's modulus of Alclad in the region from zero to about 12,000 psi compressive stress as published in reference 9.

3. In the region $\epsilon / \epsilon_{cr} > 3$ the shear modulus decreases with decreasing number of stringers.

4. The points corresponding to cylinders 26 and 30, built in the same manner with 16 stringers, follow closely the same curve. The agreement is almost as good in the case of cylinders 27, 31, and 32. These three cylinders had 12 stringers and different arrangements of the reinforcing rings. Because of these differences the buckling stress of the panels and the G_{eff} versus ϵ curves in figures 15, 19, and 20 differ considerably. At the same compressive load the value of G_{eff} is smallest for the cylinder in which the rings are not riveted to the sheet and largest for the cylinder with the closely spaced rings. However, when the experimental results are plotted in a nondimensional form as in figure 24, the points corresponding to the three cylinders follow reasonably closely one single curve.

5. In the first two preliminary tests the maximum ϵ / ϵ_{cr} ratio reached was 1.4, in the third preliminary test it was 5, and in the fourth 6.5. The experimental points corresponding to these tests are not included in figure 24. They show the same general trend as the points of the final series, but their inclusion would increase the scatter.

Cylinder 33

Cylinder 33 was built in order to extend the range of investigations to higher values of ϵ / ϵ_{cr}. Since no hard aluminum sheet thinner than 0.012 inch could be had, spring temper brass of a nominal thickness of 0.005 inch was used. Because of the small thickness of the sheet and the small width of the bands from which the cylinder had to be fabricated, the sheet covering of the cylinder was partially wrinkled even before loads were applied. Figure 25 is a photograph of cylinder 33 taken when the compressive force was about 23,000 pounds.

In order to get rid of the wrinkles application of an axial tensile load would be required. Since the state of strain under this tensile load corresponds to the state of strain at buckling, an effective strain may be defined for cylinder 33 as the measured strain augmented by the tensile strain and by the theoretical critical strain, all taken with their absolute values. In other words, when the experimental points shown in figure 21 are replotted in the nondimensional graph of figure 24, they should be shifted to the right by an amount corresponding to the sum of the absolute values of the tensile strain referred to above and the critical strain. On the other hand, the value of the former is not known. The curve representing cylinder 33 in figure 24 was therefore shifted arbitrarily until it fitted into the general pattern of the figure.

It is admitted that this procedure is rather arbitrary and thus the numerical values of the points corresponding to cylinder 33 in figure 24 are not reliable. Nevertheless, the curve is shown in the figure since it proves that the effective shear rigidity ceases to decrease even when the number of stringers is as low as 6 if only the strain is increased sufficiently.

In the calculation of the strain ratios the theoretical critical strain was used in place of the experimental critical strain because the latter was not known. The theoretical value was found to be 3.28×10^{-4} when $t = 0.0055$ inch and $E = 13.09 \times 10^{6}$ psi were used in Redshaw's formula (equation (4)). The value of Young's modulus was taken from reference 12. A tensile test made with a strip of the brass sheet to which metalectric strain gages were cemented checked the handbook value within 3.9 percent. In the computation of

the shear modulus ratio $G_o = 5.12 \times 10^6$ psi was used. This was also taken from reference 12.

Presentation of the Results

The following empirical formula is suggested as a representation of the variation of the effective shear modulus with compressive strain:

$$\frac{G_{eff}}{G_o} = (1 - N)e^{-N(\epsilon / \epsilon_{cr})} + N \qquad (12)$$

$$N = 0.0275[(2\pi r/d) + 1] \qquad (12a)$$

The four curves shown in figure 26 were calculated from this formula for the values $n = (2\pi r/d) = 6$, 8, 12, and 16. Comparison of figures 24 and 26 discloses good general agreement for values of ϵ / ϵ_{cr} greater than 3, except that the formula gives higher values for G/G_{eff} than those shown in figure 24 when $n = 6$ and ϵ / ϵ_{cr} is large. This deviation is intentional, since no full credence should be given to the values obtained with cylinder 33. In the region where ϵ / ϵ_{cr} is less than 3 the indicental variations of the experimental curves caused by the unpredictable behavior of Alclad are not followed by the empirical formula.

Failure of the Cylinders

All the cylinders of the final test series failed in buckling of the panel type. Figure 27 shows cylinder 27 after its stringers buckled in the top and bottom panels. The failing loads and failing strains are listed in table 3.

The failure of the first three preliminary test cylinders was not due to compression but rather to bending as described in reference 7. The fourth preliminary test cylinder failed in general instability of the inward bulge type under a load of 44,500 pounds. The bulge involved 3 stringers and

2 rings. The buckled cylinder is shown in figure 28. The greatest measured compressive load was 45,500 pounds, which corresponded to an average strain of about 18×10^{-4}. The maximum strain measured in the stringer at the middle of the bulge was 20.9×10^{-4}. The greatest strain measured in the monocoque was 23.7×10^{-4}. It was obtained in a stringer at 90° from the middle of the bulge when the total compressive load was 44,150 pounds.

It is interesting to compare the average strain observed at buckling with the critical strain predicted by the theory of general instability in pure bending. Such a comparison was carried out with the aid of the formulas developed in reference 13. It was found that the use of $n = 2.21$ in the buckling formula resulted in agreement between observed and calculated critical strain. With this value of n the inward bulge would extend over 4 to 5 rings and 8 stringers according to the theory valid for pure bending.

Obviously, the theory discussed in reference 12 does not hold in the case of pure compression. Nevertheless, it is worthwhile to know that the value of n must be chosen considerably smaller than in the case of pure bending if it is applied to the case of pure compression in order to obtain a rough approximation. This result might be anticipated because of the absence of the support contributed by the tension side of the cylinder in the case of pure bending.

CONCLUSIONS

The shearing rigidity of a circular cylindrical panel decreases when increasing amounts of compressive loads are applied to the panel in the axial direction. In many calculations it is convenient to take this decreased rigidity into account by the use of an effective shear modulus G_{eff}. The results of tests carried out with reinforced monocoque cylinders made of Alclad sheet are shown in the nondimensional plot of figure 24. On the basis of this figure the following empirical formula was established:

$$\frac{G_{eff}}{G_o} = (1 - N)e^{-N(\epsilon / \epsilon_{cr})} + N \qquad (12)$$

where

$$N = 0.0275[(2\pi r/d) + 1] \qquad (12a)$$

The curves represented by this formula are plotted in figure 26 for the cases of 6, 8, 12, and 16 stringers.

The formula was developed from data obtained from tests carried out in the following approximate range of the parameters:

$$0 < \epsilon/\epsilon_{cr} < 12$$

$$1 < r/d < 2.5$$

Equation (12) should be used with caution when the parameters are outside of this range.

Polytechnic Institute of Brooklyn,
Brooklyn, N. Y., August, 1945.

REFERENCES

1. Hoff, N. J., Boley, Bruno A., and Klein, Bertram: Stresses in and General Instability of Monocoque Cylinders with Cutouts. II - Calculation of the Stresses in a Cylinder with a Symmetric Cutout. NACA TN No. 1014 (to be published).

2. Hoff, N. J., and Boley, Bruno A.: Stresses in and General Instability of Monocoque Cylinders with Cutouts. I - Experimental Investigation of Cylinders with a Symmetric Cutout Subjected to Pure Bending. NACA TN No. 1013 (to be published).

3. Hoff, N. J., and Klein, Bertram: The Inward Bulge Type Buckling of Monocoque Cylinders. III - Revised Theory Which Considers the Shear Strain Energy. NACA TN No. 968, 1945.

4. Kuhn, Paul, and Chiarito, Patrick T.: Shear Lag in Box Beams. Methods of Analysis and Experimental Investigations. Rep. No. 739, NACA, 1942.

5. Kuhn, Paul: A Procedure for the Shear-Lag Analysis of Box Beams. NACA ARR, Jan. 1943.

6. Hoff, N. J.: General Instability of Monocoque Cylinders. Journal of the Aeronautical Sciences, Vol. 10, No. 4, pp. 105-114, 130, April 1943.

7. Hoff, N. J., Fuchs, S. J., and Cirillo, A. J.: The Inward Bulge Type Buckling of Monocoque Cylinders. Part II - Experimental Investigation of the Buckling in Combined Bending and Compression. NACA TN No. 939, 1944.

8. Ebner, H.: The Strength of Shell Bodies - Theory and Practice. NACA TM No. 838, 1937.

9. Templin, R. L., Hartmann, E. C., and Paul, D. A.: Typical Tensile and Compressive Stress-Strain Curves for Aluminum Alloy 24S-T, Alclad 24S-T, 24S-RT, and Alclad 24S-RT Products. Technical Paper No. 6, Aluminum Res. Lab., Aluminum Company of America, 1942.

10. Timoshenko, S.: Theory of Plates and Shells. 1st ed. McGraw-Hill Co., 1940.

11. Sokolnikoff, Ivan S. and Sokolnikoff, Elizabeth S.: Higher Mathematics for Engineers and Physicists. 2d ed., McGraw-Hill Co., 1941, p. 544.

12. Hodgman, Charles D.: Handbook of Chemistry and Physics. 22d ed. Chemical Rubber Publishing Co., 1937.

13. Hoff, N. J., and Klein, Bertram: The Inward Bulge Type Buckling of Monocoque Cylinders. I - Calculation of the Effect upon the Buckling Stress of a Compressive Force, a Nonlinear Direct Stress Distribution, and a Shear Force. NACA TN No. 938, 1944.

APPENDIX

A small error was introduced in the calculations when the sheet covering alone was assumed to resist torsion. The order of magnitude of this error will now be determined.

The geometric factor C in the torsional rigidity GC of a thin-walled circular cylinder is given by

$$C = 4A^2t/S = 2\pi r^3t$$

In the case of cylinder 10

$$C = 75 \text{ in.}^4$$

The geometric factor C in the torsional rididity GC of a solid square section of edge length a is

$$C = 0.14\ a^4$$

For a stringer of 3/8 in. square section

$$C = 0.00277 \text{ in.}^4$$

For 16 stringers $16 \times 0.00277 = 0.0443$ in.^{4}, which is about 0.06 percent of the value of C for the sheet alone.

When the monocoque is twisted, the stringers are bent as well as twisted. A rough calculation of the increase in the torsional rigidity of cylinder 10 because of the bending of the stringers can be carried out as follows:

In the case of a rotation of 0.01 radian the relative tangential displacement of the two end points of a stringer is 0.1 in. If the ends of the stringer are assumed to be rigidly fixed to the end rings, the force Q needed to cause such a displacement is $(12\ EI/L^3) \times 0.1$ lb. With

$I = 0.00165$ in.^{4}

$$Q = 0.77 \text{ lb.}$$

The torque T_1 caused by the forces Q acting upon all the 16 stringers is

$$T_1 = 123 \text{ in.-lb.}$$

On the other hand, if the sheet alone is taken into account, the torque T_2 necessary to twist cylinder 10 is

$$T_2 = (GC/L) \times 0.01 = 95{,}000 \text{ in.-lb.}$$

Consequently T_1 is only about 0.1 percent of T_2.

Finally, the compression load bar had also to be twisted in all the tests of cylinders 7, 8, and 10. Factor C for a solid circular section is equal to the polar moment of inertia. Since the diameter D of the load bar was 1.25 in.,

$$C = I_p = (\pi/32) D^4 = 0.239 \text{ in.}^4$$

This amounts to about 0.3 percent of the value of C found for the thin-walled cylinder. The percentage so obtained should be multiplied, however, by approximately 3 since the compression load bar is of steel, while the cylinder is of aluminum alloy.

In conclusion, it may be stated that the simple formula used in this report for the calculation of the effective shear modulus is accurate enough for practical purposes.

Table 1.- Cylinder Characteristics

Cyl. No.	No. of Stringers $n = \frac{2\pi r}{d}$	Diameter in.	$\frac{r}{d}$	Sheet thickness in.	Ring Spacing in.	Ring Cross-section	Fasteners for Stringers	Fasteners for Rings	Sheet Material	Stringer Material	$K = \frac{LS}{4A^2t}$ in.$^{-3}$
						Final Test Series					
26	16	16	2.55	0.012	4.5	3/8"x3/8"	Rivets	Rivets	24 ST alclad	24 ST aluminum alloy	.348
27	12	16	1.91	0.012	4.5	"	Rivets	Rivets			.348
28	8	16	1.27	0.012	4.5	"	Rivets	Rivets			.348
29	6	16	0.95	0.012	4.5	"	Rivets	Rivets			.346
30	16	16	2.55	0.012	4.5	"	Rivets	Rivets			.348
31	12	16	1.91	0.012	4.5	"	Rivets	———			.347
32	12	16	1.91	0.012	2.57	"	Rivets	Rivets			.327
33	6	16	0.95	0.0055	4.5	"	Screws	Screws	Spring Temper Brass 72% Cu 28% Zn		.758
						Preliminary Test Series					
7	16	20	2.55	0.020	5	1/8"x3/8	Screws	———	24 ST aluminum alloy	17ST aluminum alloy	.226
8	16	20	2.55	0.020	5	"	Screws	———			.226
10	16	20	2.55	0.012	5	"	Screws	———	24 ST alclad		.416
15	16	16	2.55	0.012	5	"	Screws	———		24ST al.alloy	.420

For all cylinders: Stringer Section: 3/8" x 3/8". Ring Material: 24ST aluminum alloy. 1/8" machine screws for fastening stringers and rings at their intersection.

Table 2.- Buckling of Sheet Covering

Cylinder Number	Buckling observed $\epsilon_{cr} \times 10^4$	Strain ϵ_{cr} theoretical $\times 10^4$	Maximum ϵ/ϵ_{cr} reached in test based on observed ϵ_{cr}
	Final Test Series		
26	3.0	4.46	10.87
27	3.0	4.42	10.58
28	2.5	4.18	12.23
29	3.3	4.15	10.00
30	5.0	4.46	6.84
31	2.2	4.27	13.55
32	4.0	4.54	10.54
33	—	3.28	—
	Preliminary Test Series		
7	4.73	6.00	1.13
8	3.81	6.00	1.49
10	1.48	3.60	5.04
15	2.76	4.42	6.65

The theoretical value of ϵ_{cr} was calculated from Redshaw's formula (equation 4).

Table 3.- Failure of Cylinders

Cylinder Number	Type of Failure	Maximum Compressive Load P lb.	Maximum Stringer Strain (average) $\times 10^4$	Maximum Stringer Stress (average) p.s.i.
		Final Test Series		
26	Panel type buckling	78,800	33.75	33,500
27		61,150	35.50	35,200
28		40,600	33.60	33,400
29		30,800	35.25	35,000
30		82,000	34.80	34,600
31		60,900	33.80	33,600
32		70,390	48.40	45,000
33		23,800	33.20	33,000
		Preliminary Test Series		
7, 8, 10	Failure described in Reference 7.			
15	General instability	45,500	18.00	18,900

Fig. 1

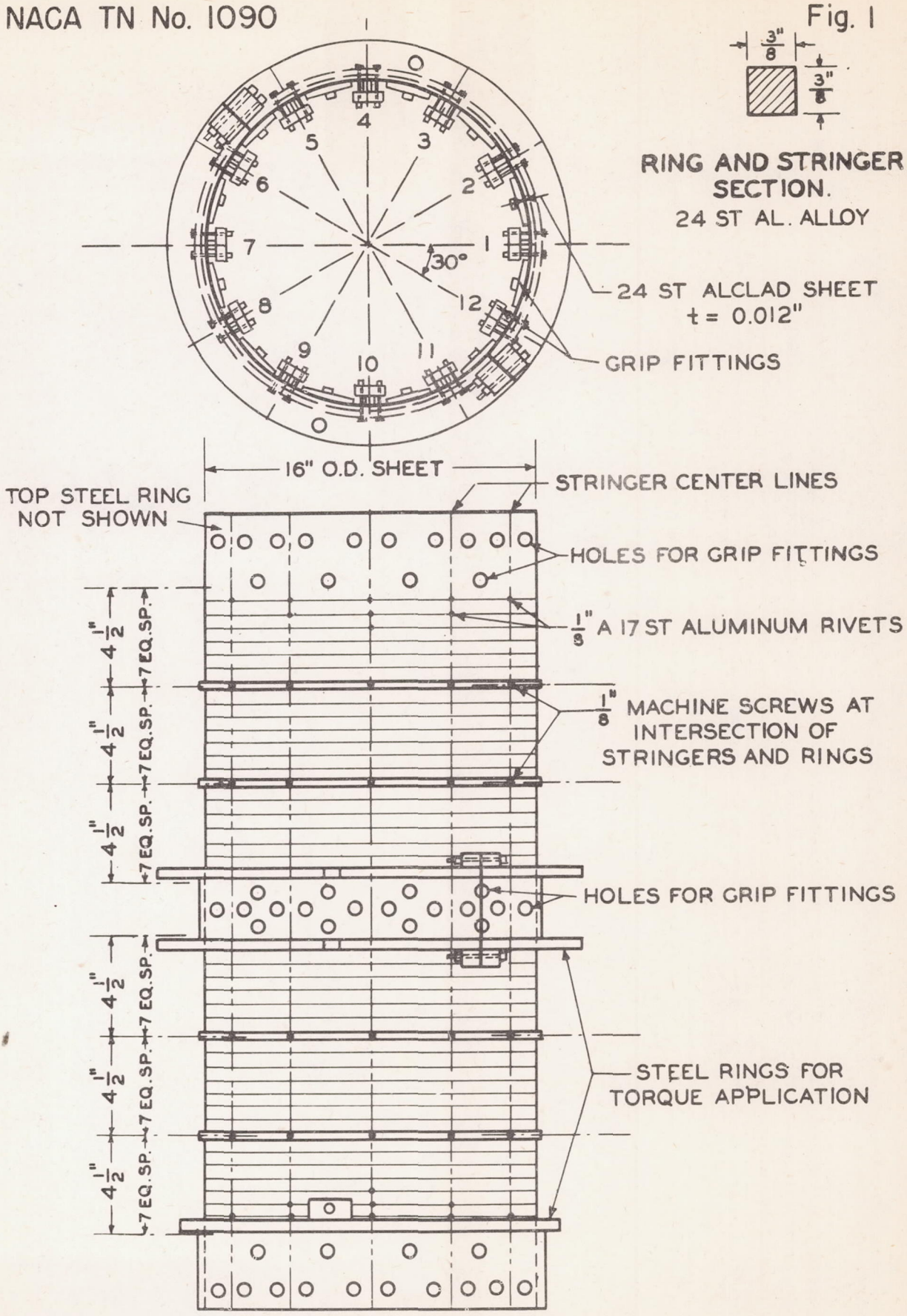


FIG. 1.- TYPICAL TEST SPECIMEN FOR FINAL SERIES OF TESTS.

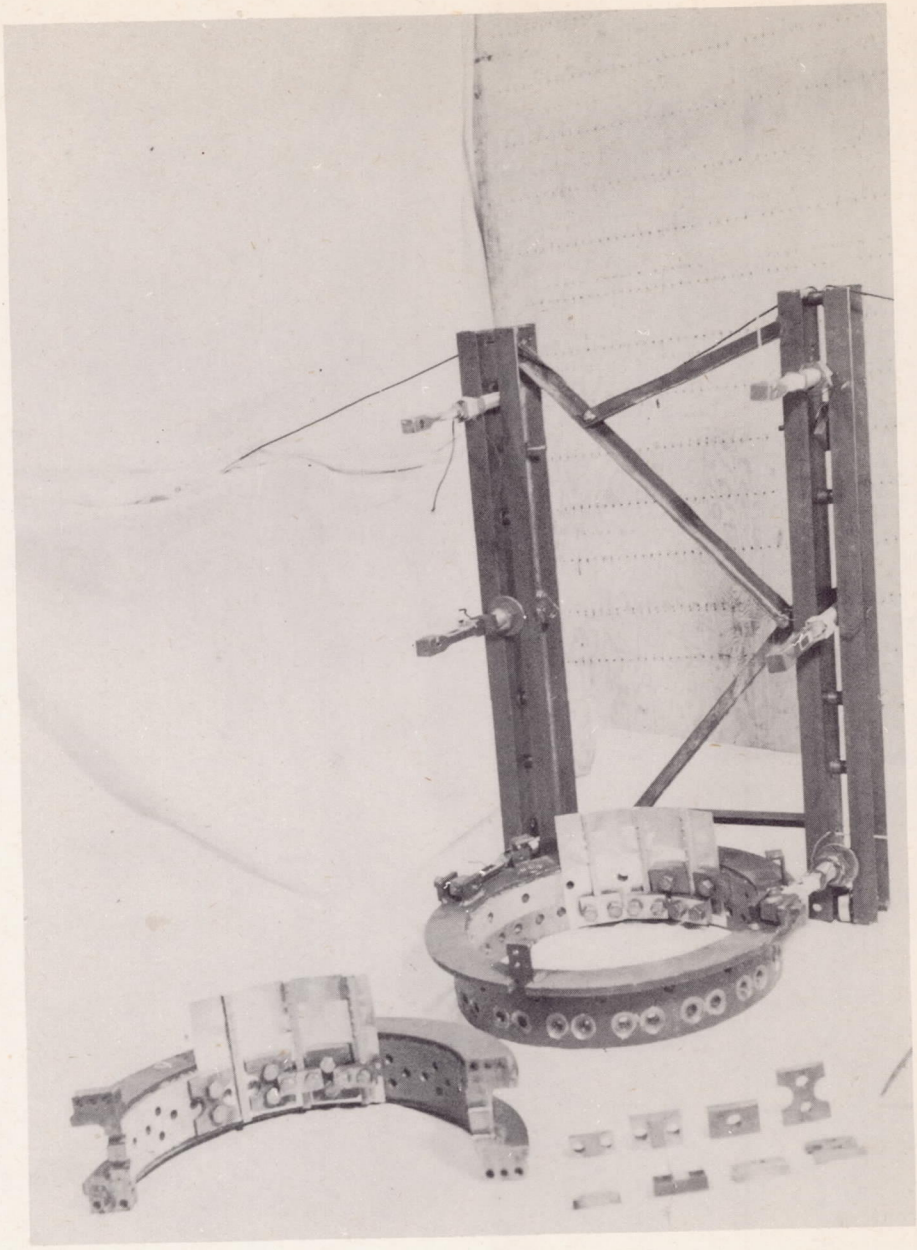


Figure 2.- Details of torsion loading apparatus for final series of tests. The links for the application of the torque are shown attached to the loading frame. The two lower links are connected to the bottom steel ring. One half of the middle steel ring lies on the left. Portions of the sheet covering and stringers are shown attached to each steel ring by means of grip fittings. Two of each type of grip fittings are in the foreground, in the following order, from left to right: stringer grip fittings for middle and end rings, sheet grip fittings for end and middle rings, respectively.

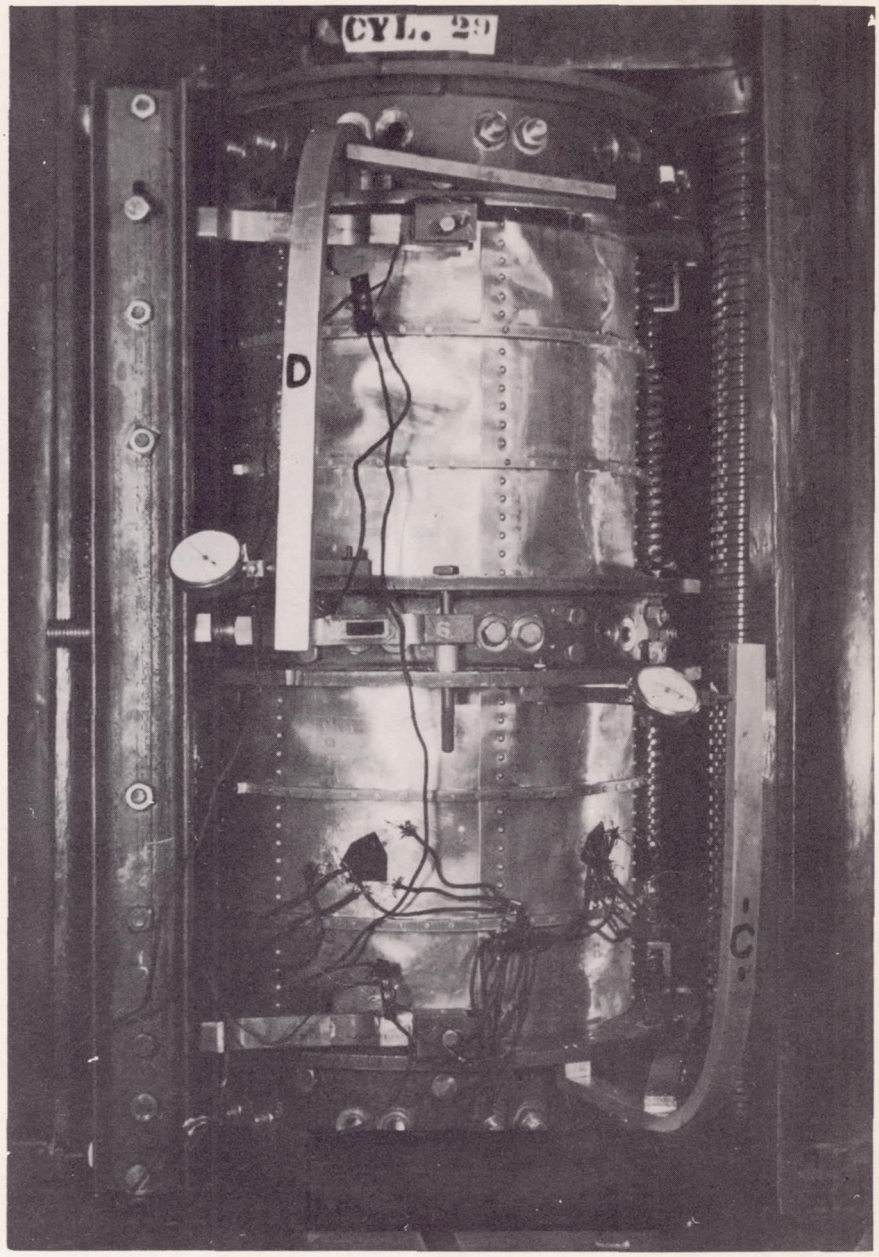
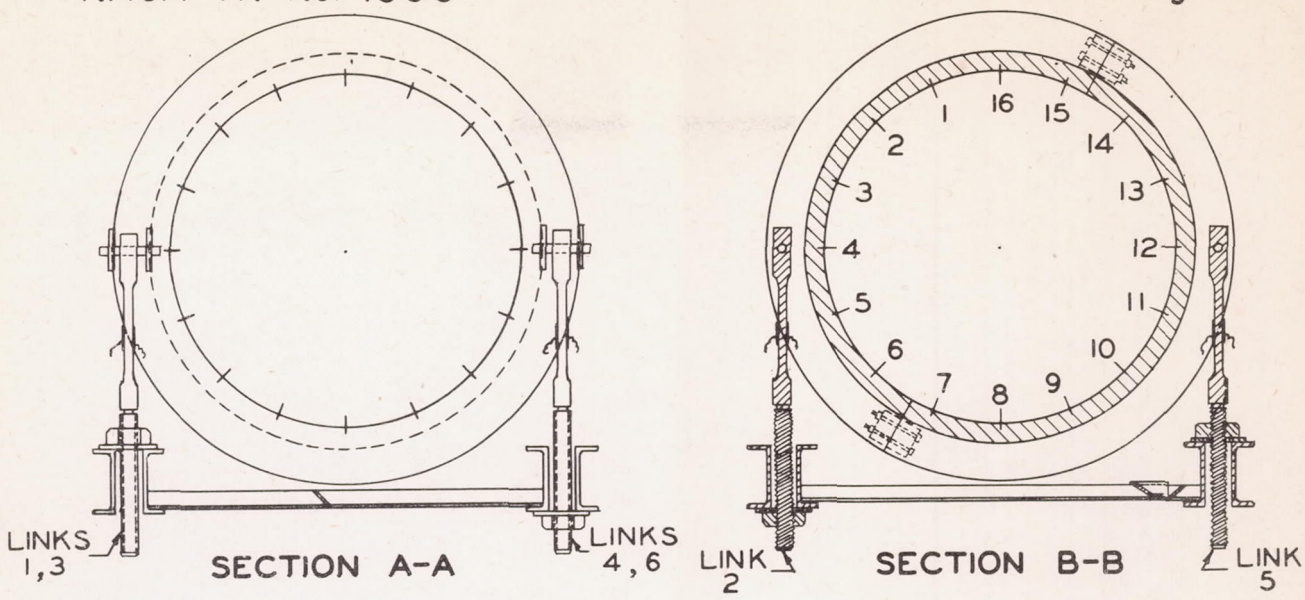


Figure 3.- Cylinder 29 under load. P = 20,000 lb.



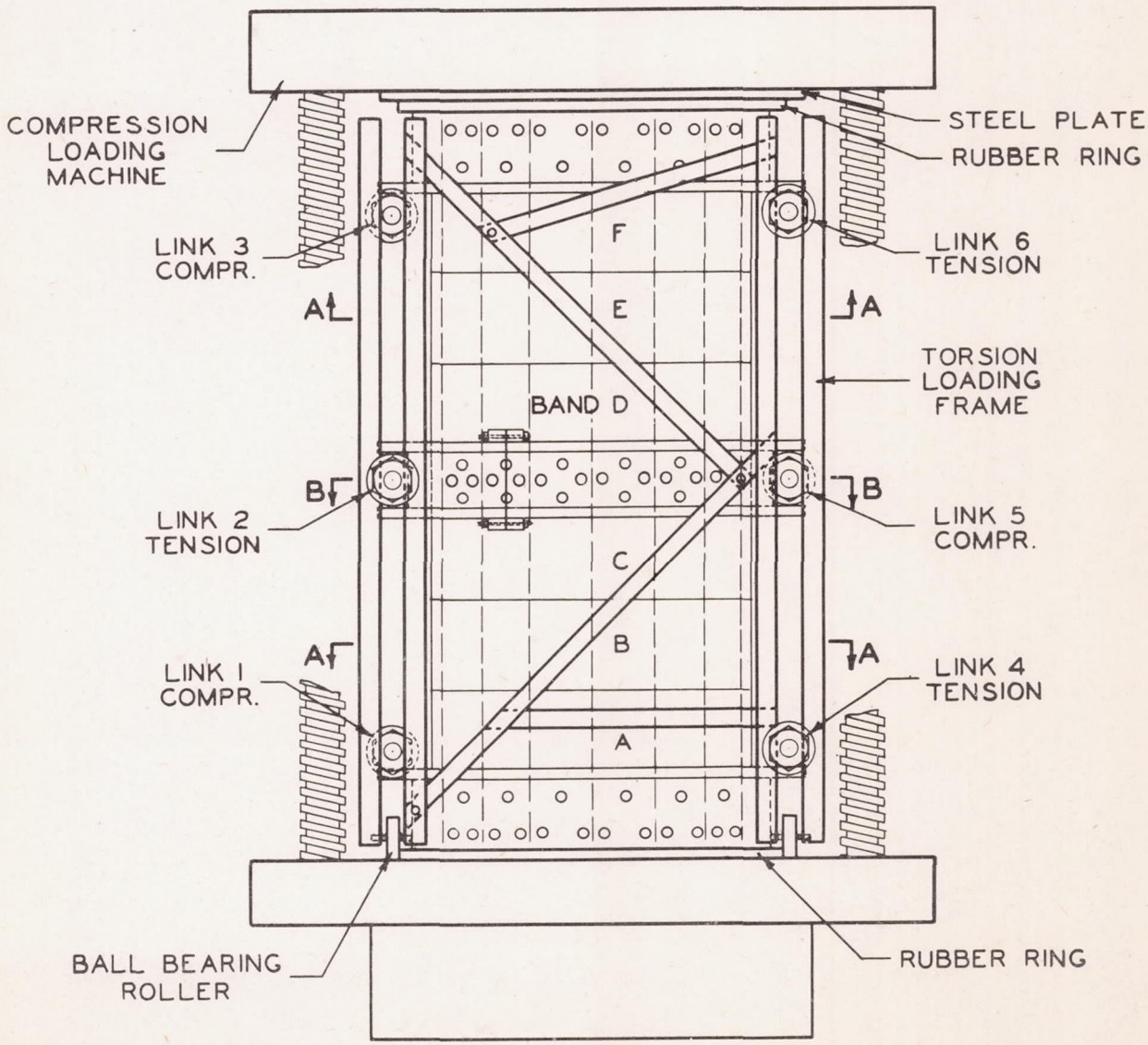


FIG. 4.- SET-UP FOR FINAL SERIES OF TESTS.

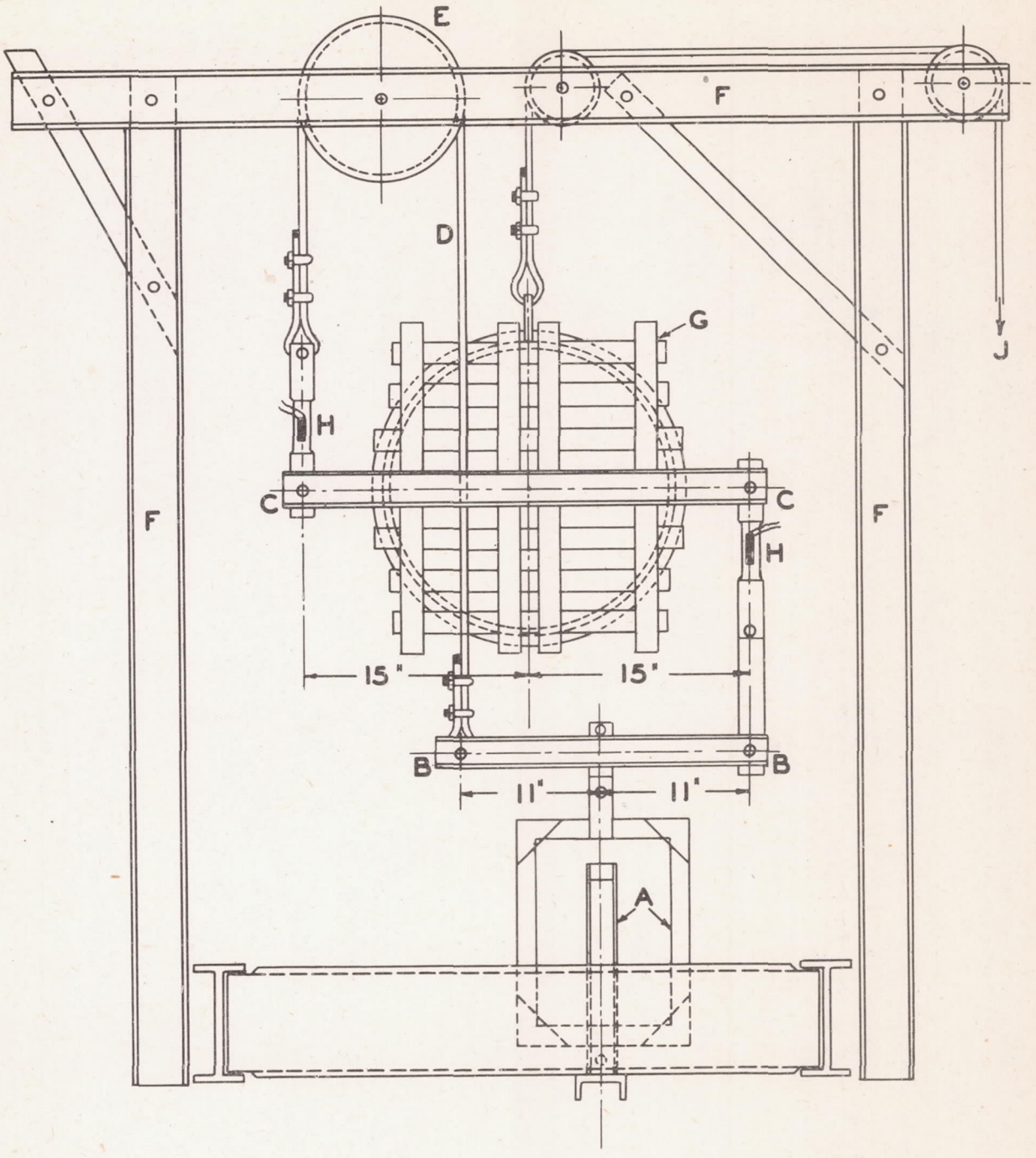


FIG. 5.–TORQUE APPLICATION FOR CYLINDERS 7, 8 AND 10 OF PRELIMINARY SERIES OF TESTS.

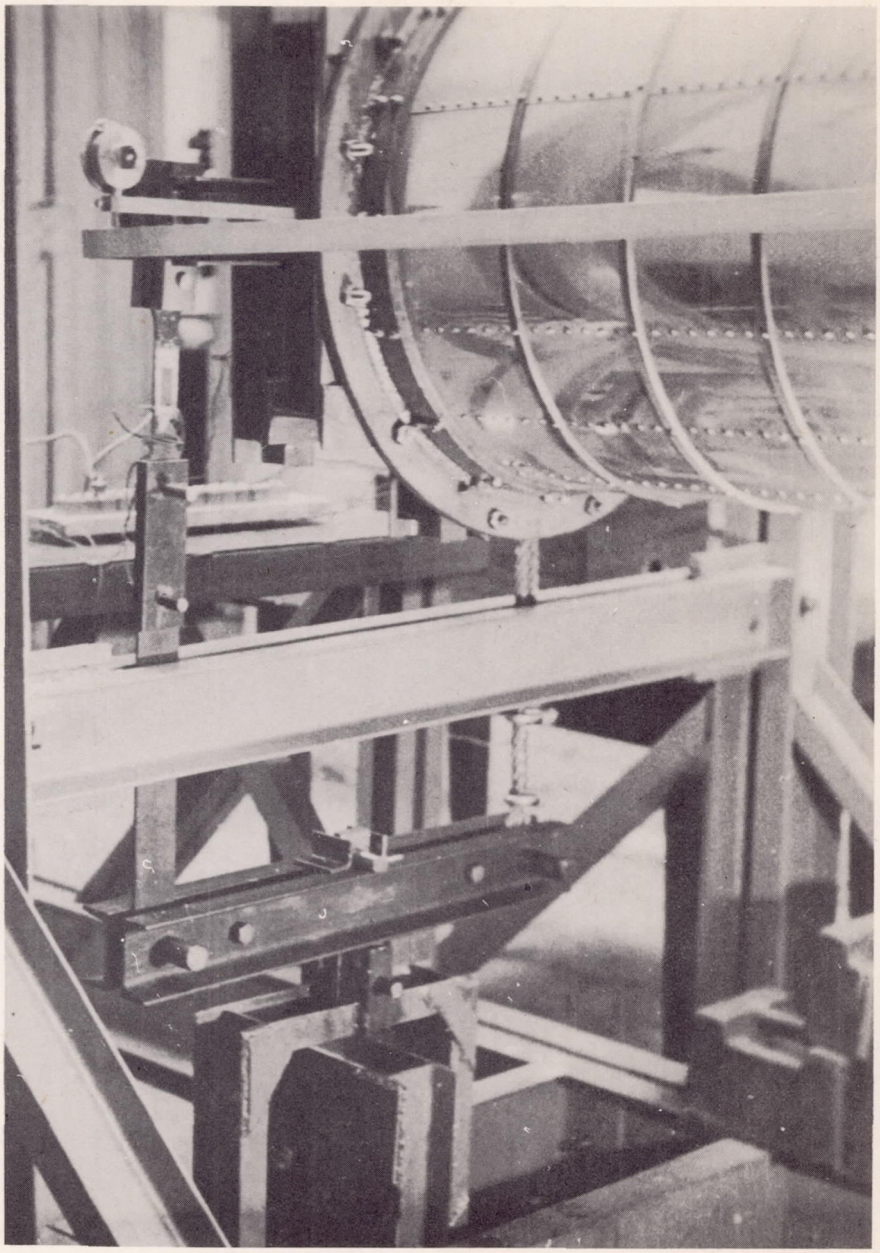


Figure 6.- Torque application for cylinders 7, 8, and 10 of the preliminary series of tests.

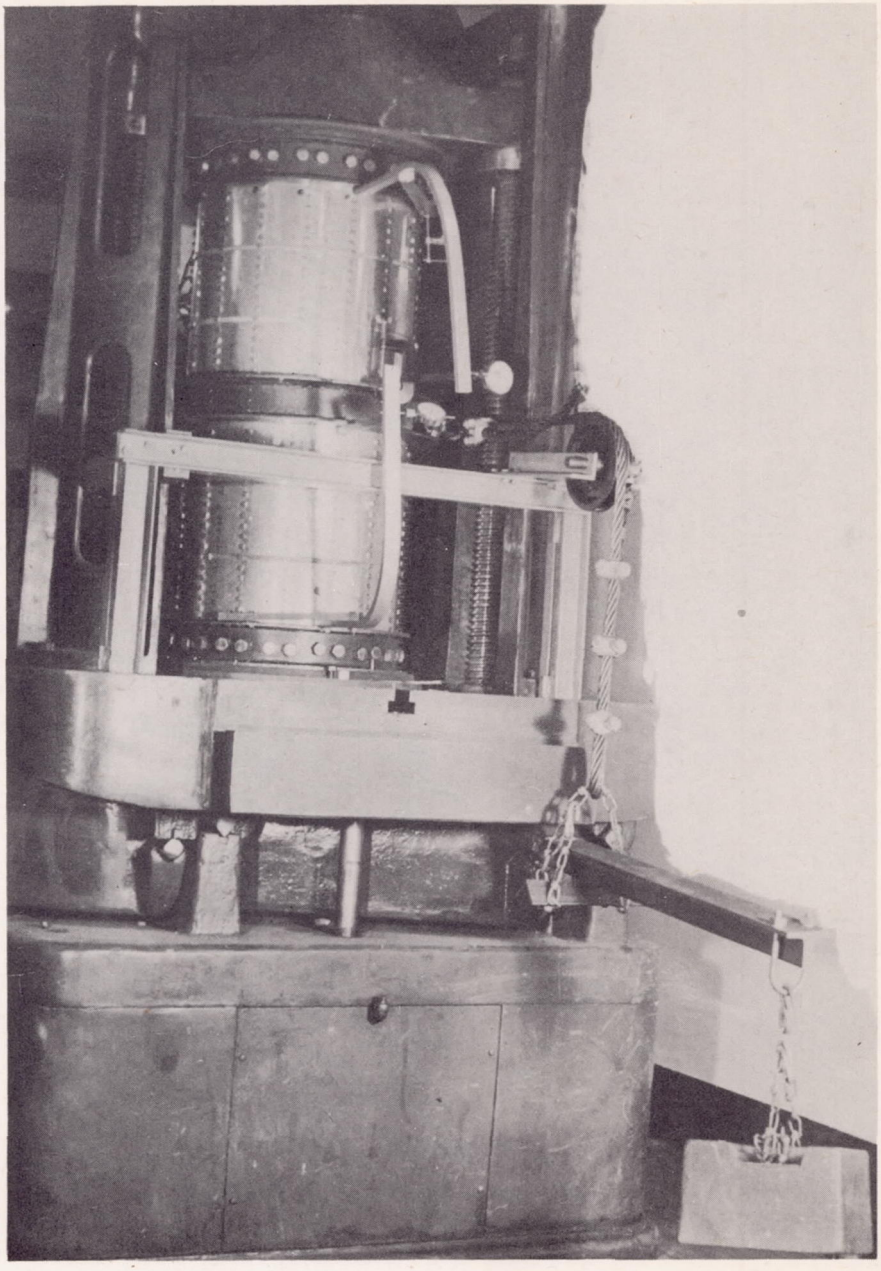


Figure 7.- Test set-up for cylinder 15 of the preliminary series of tests.

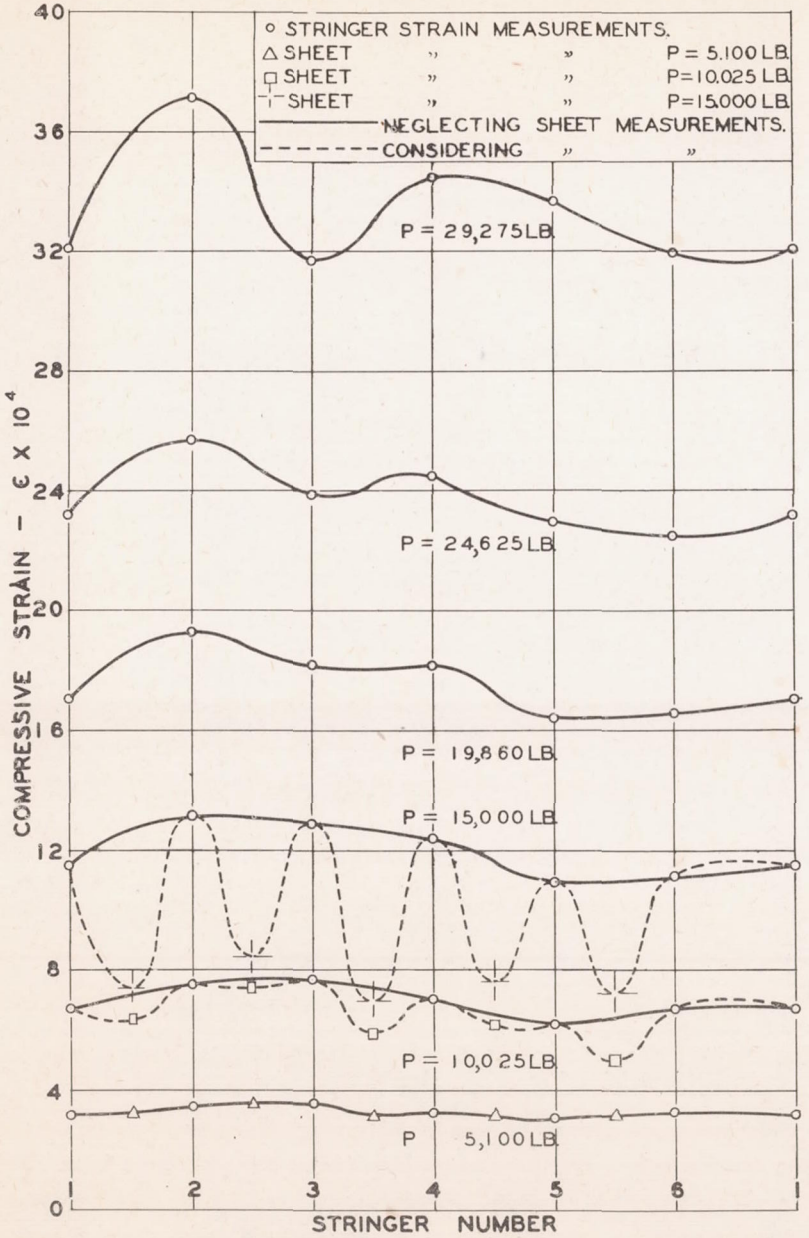


FIG. 8.- DISTRIBUTION OF STRAIN IN COMPRESSION
CYL. 29 BAND B

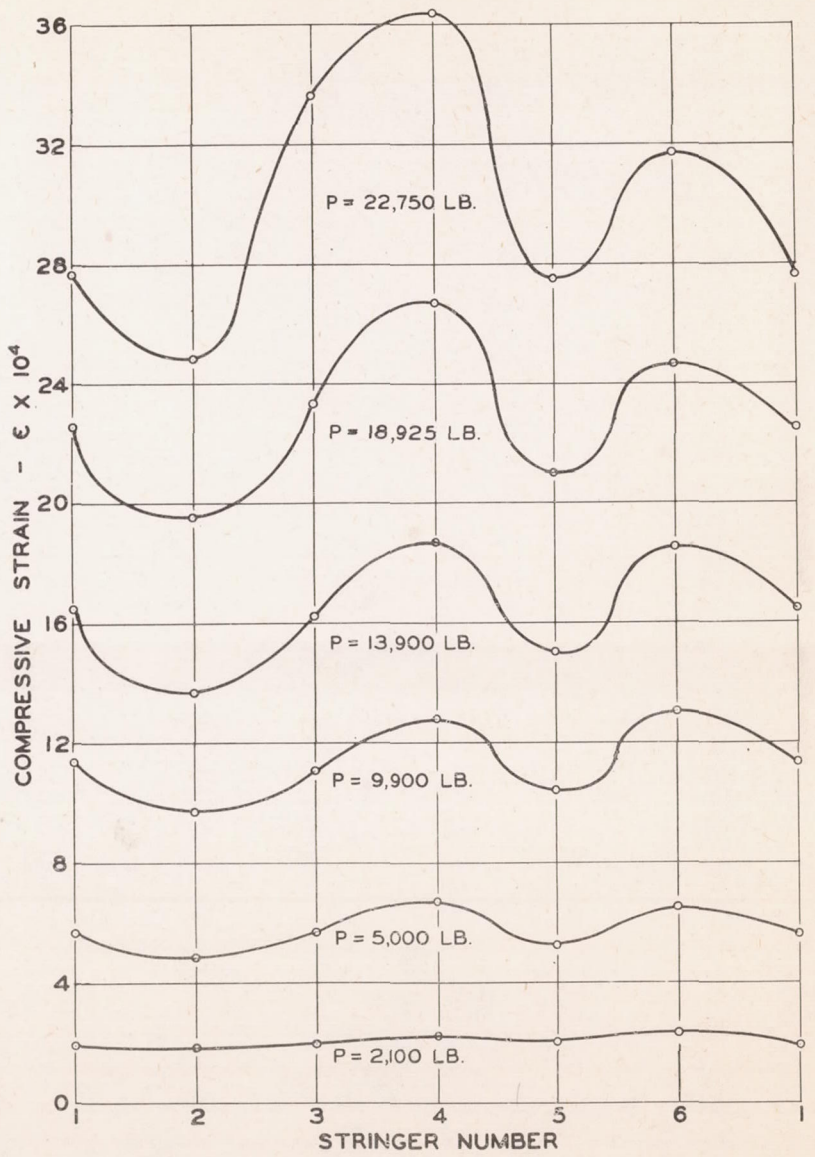


FIG. 9.- DISTRIBUTION OF STRAIN IN COMPRESSION.
CYL. 33 BAND E

Figs. 8,9

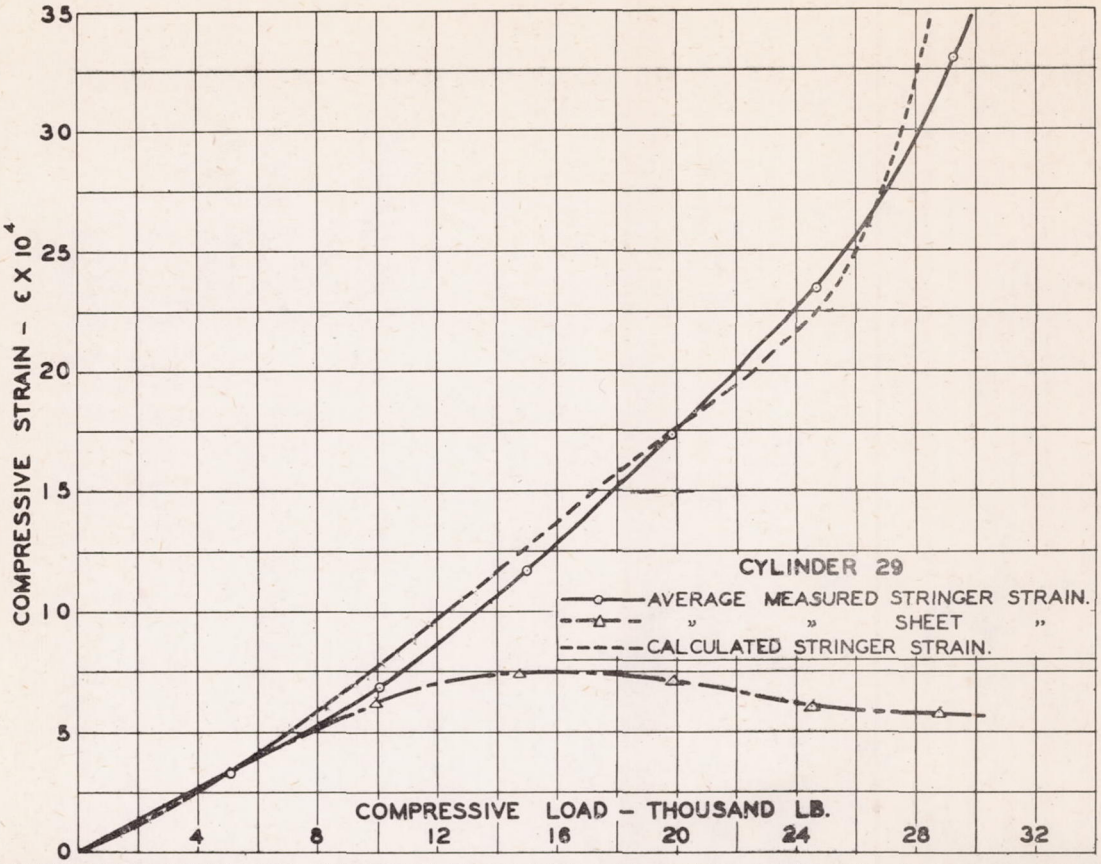


FIG. 10.- VARIATION OF COMPRESSIVE STRAIN WITH APPLIED COMPRESSIVE LOAD

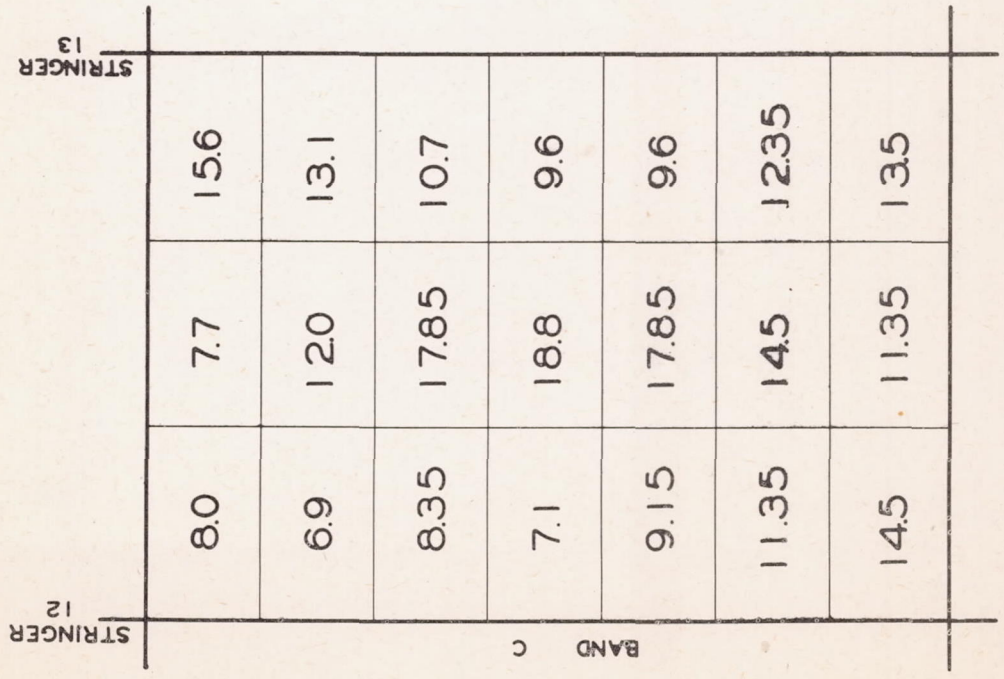


FIG. 11.- RADIUS OF CURVATURE OF TYPICAL PANEL
CYLINDER 30
RADIUS GIVEN IN INCHES

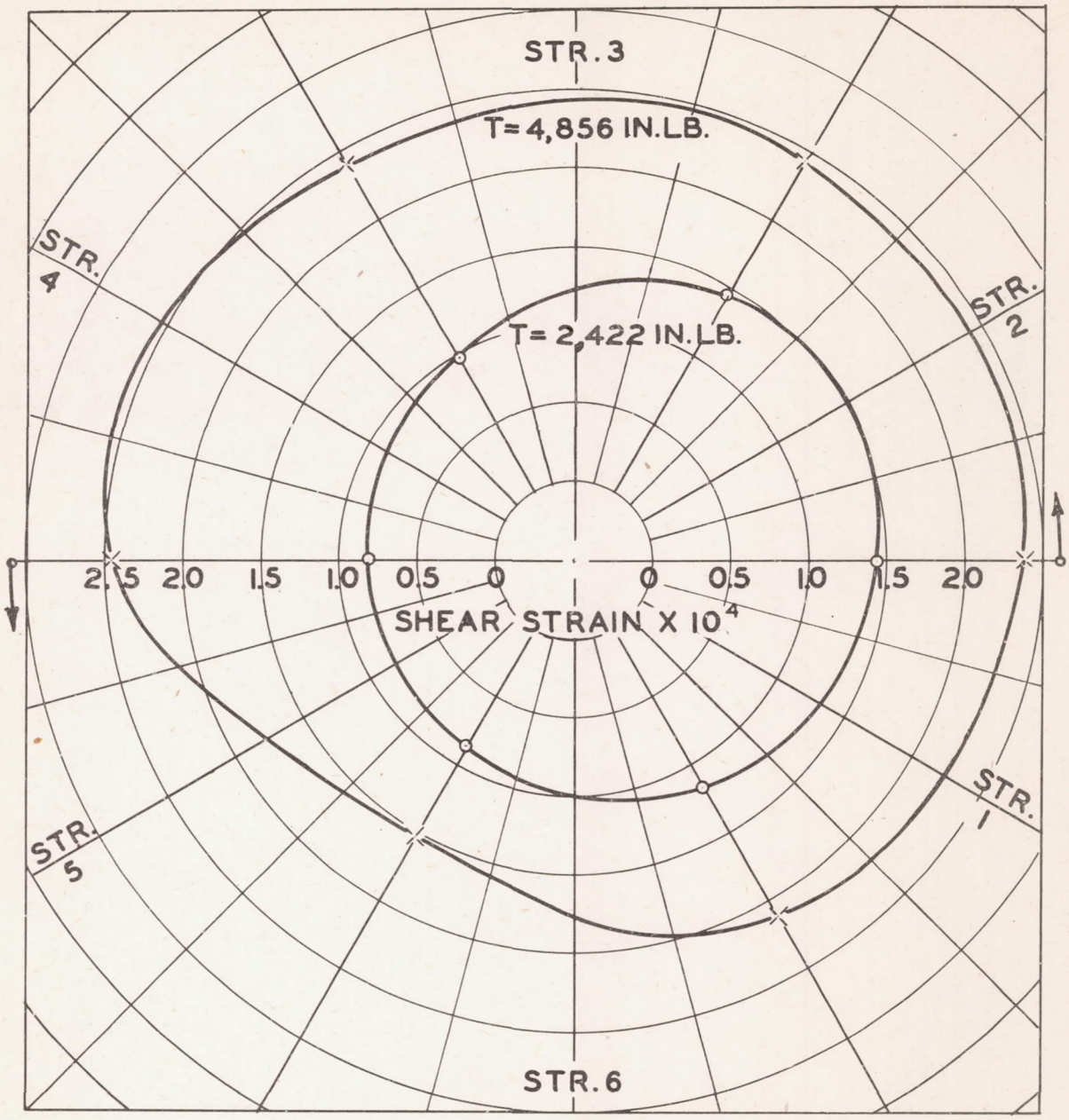


FIG. 12.- SHEAR STRAIN DISTRIBUTION IN THE SHEET DUE TO TORSION.

TORQUE APPLICATION SHOWN BY ARROWS.

CYLINDER 29 P = 0 LB.

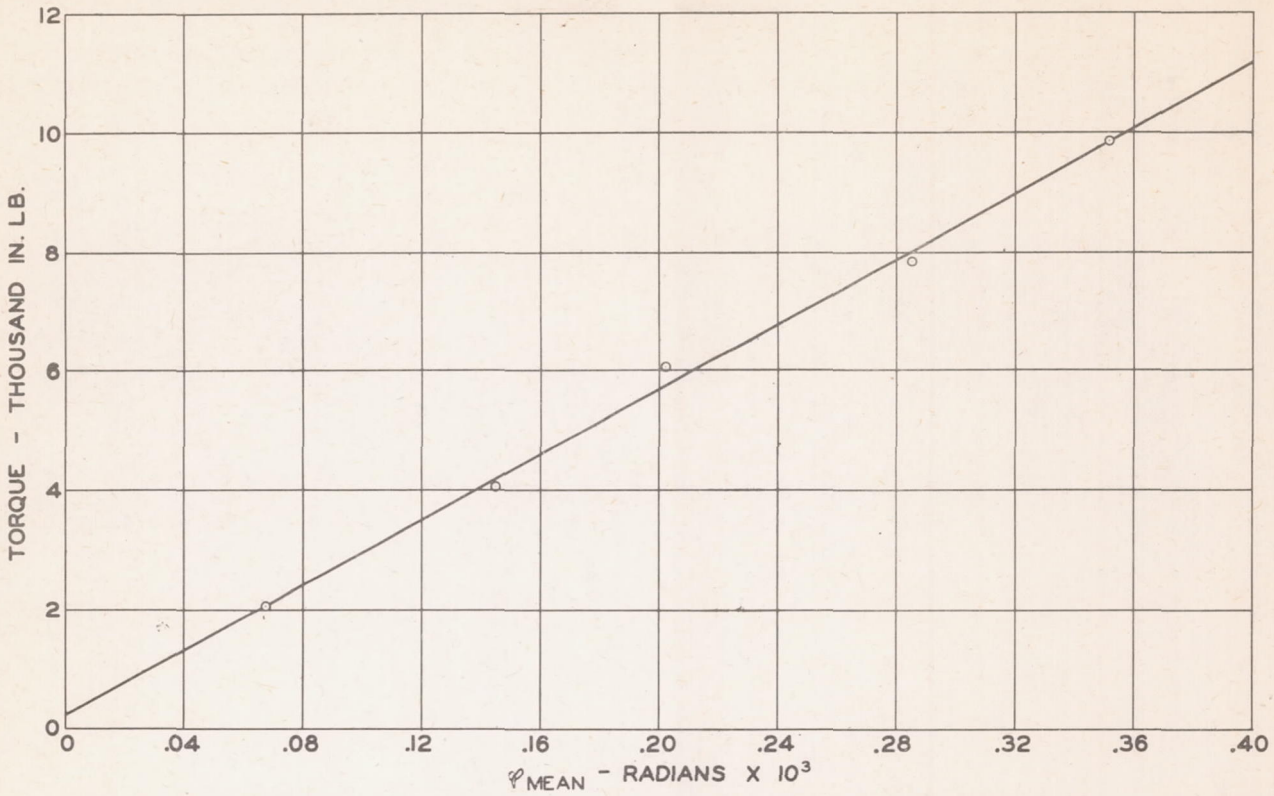


FIG. 13.- VARIATION OF MEAN ANGLE OF TWIST WITH APPLIED TORQUE.
CYL. 26 P = 24,350 LB.

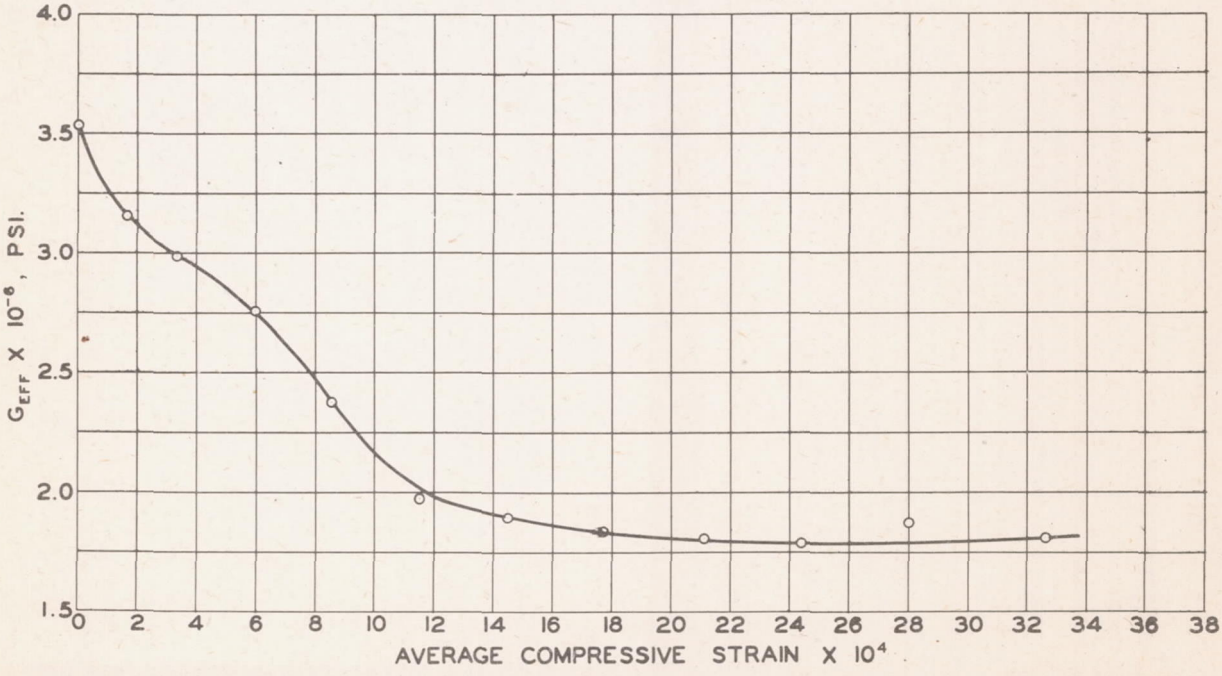


FIG. 14.- VARIATION OF EFFECTIVE SHEAR MODULUS G_{EFF} WITH AVERAGE COMPRESSIVE STRAIN.

CYLINDER 26

DIAMETER D = 16" 16 STRINGERS RING SPACING 4.5"
SHEET THICKNESS t = 0.012" SHEET MATERIAL 24 ST ALCLAD

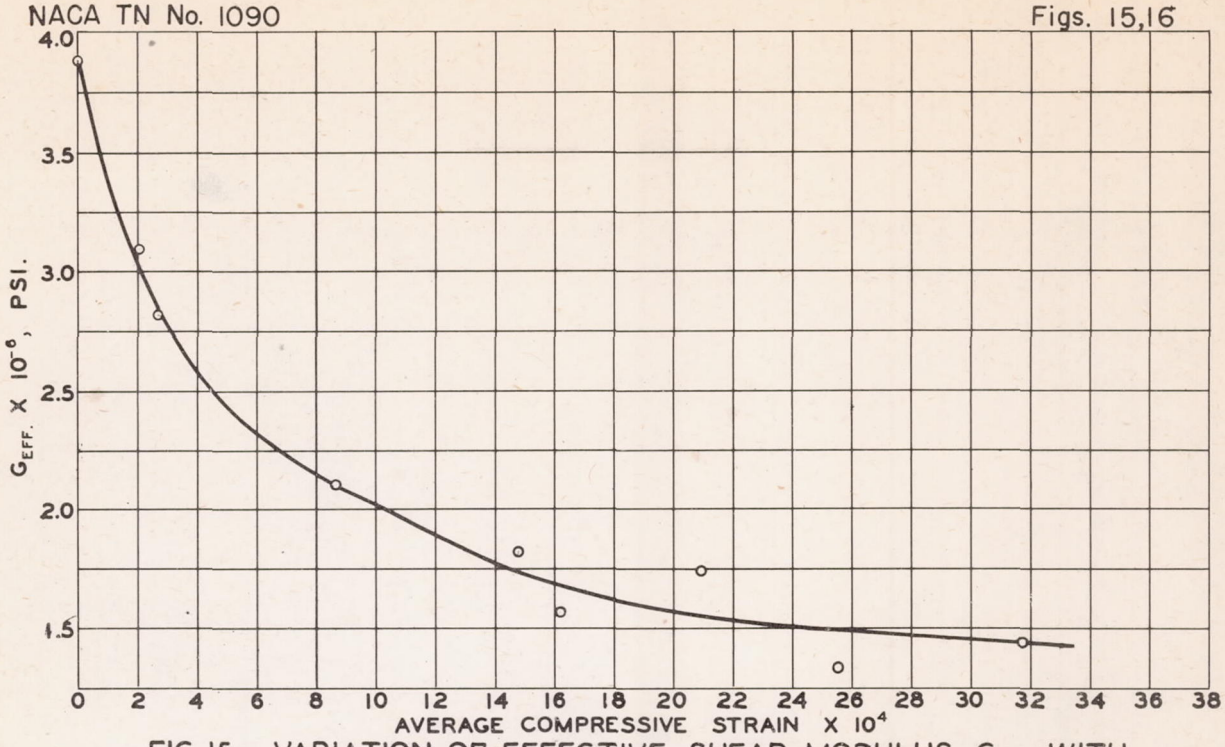


FIG. 15.- VARIATION OF EFFECTIVE SHEAR MODULUS $G_{EFF.}$ WITH AVERAGE COMPRESSIVE STRAIN.

CYLINDER 27

DIAMETER D = 16" 12 STRINGERS RING SPACING 4.5"
SHEET THICKNESS t = 0.012" SHEET MATERIAL 24 ST ALCLAD

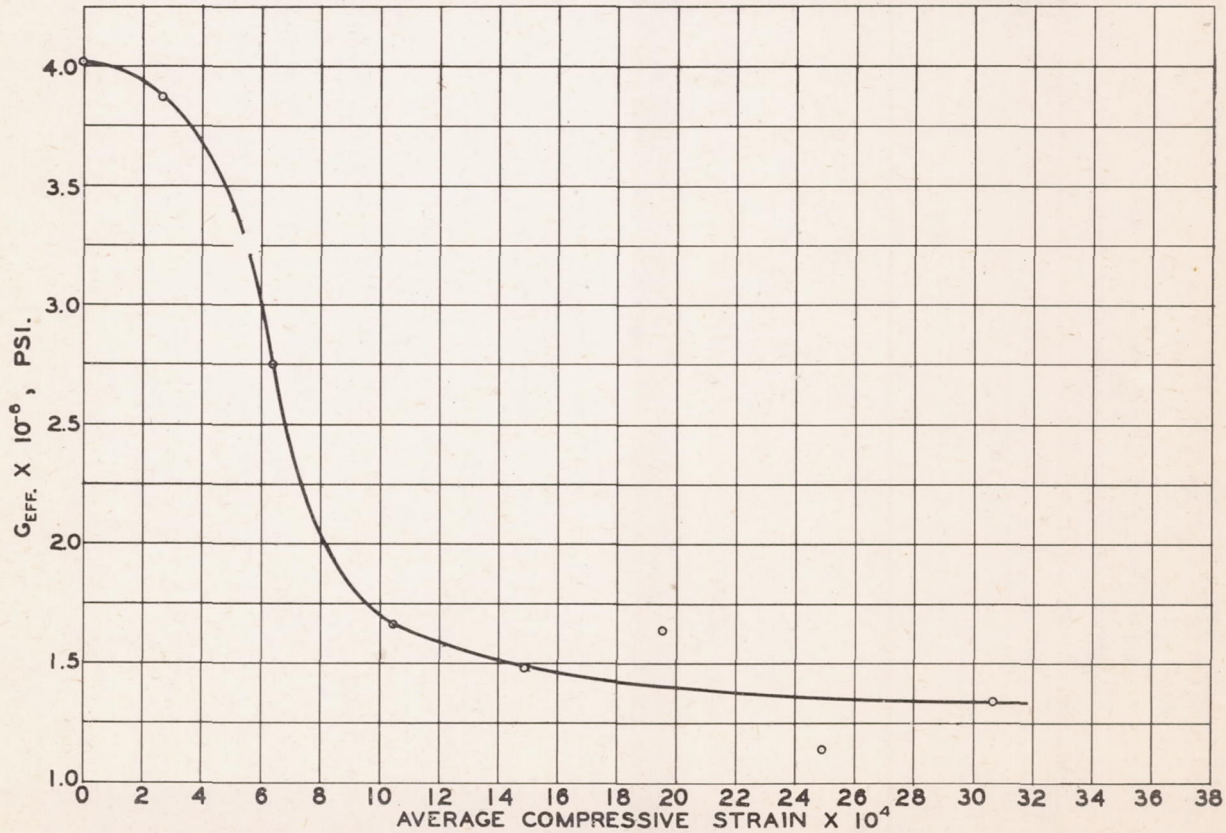


FIG. 16.- VARIATION OF EFFECTIVE SHEAR MODULUS $G_{EFF.}$ WITH AVERAGE COMPRESSIVE STRAIN.

CYLINDER 28

DIAMETER D = 16" 8 STRINGERS RING SPACING 4.5"
SHEET THICKNESS t = 0.012" SHEET MATERIAL 24 ST. ALCLAD.

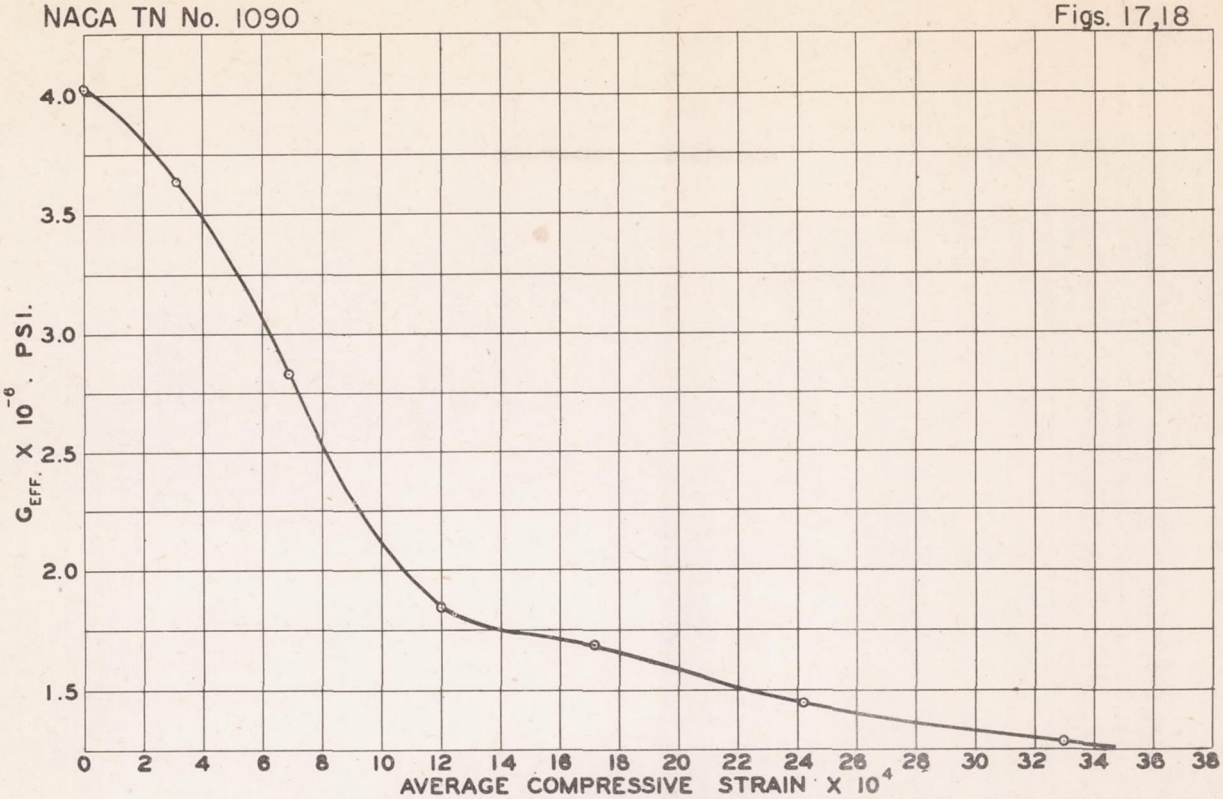


FIG. 17.- VARIATION OF EFFECTIVE SHEAR MODULUS $G_{EFF.}$ WITH AVERAGE COMPRESSIVE STRAIN

CYLINDER 29

DIAMETER D = 16" 6 STRINGERS RING SPACING 4.5"
SHEET THICKNESS t = 0.012" SHEET MATERIAL 24 ST ALCLAD

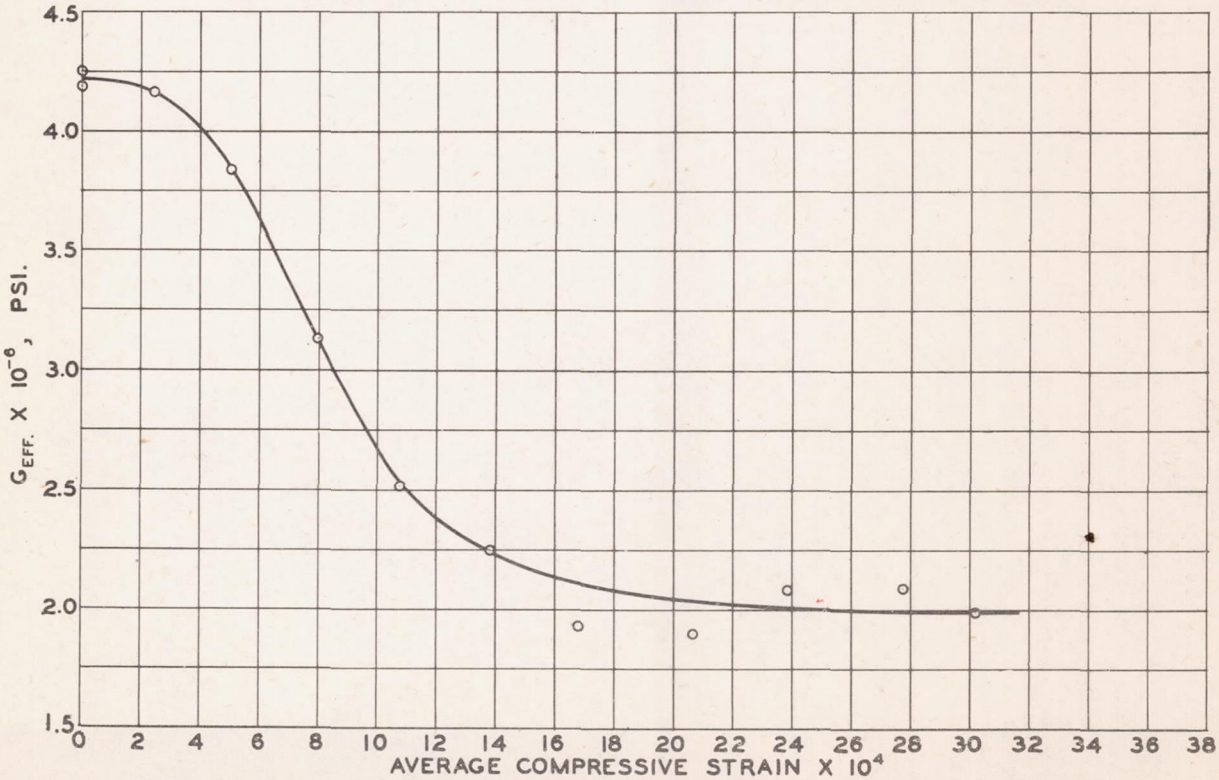


FIG. 18.- VARIATION OF EFFECTIVE SHEAR MODULUS $G_{EFF.}$ WITH AVERAGE COMPRESSIVE STRAIN

CYLINDER 30

DIAMETER D = 16" 16 STRINGERS RING SPACING 4.5"
SHEET THICKNESS t = 0.012" SHEET MATERIAL 24 ST. ALCLAD.

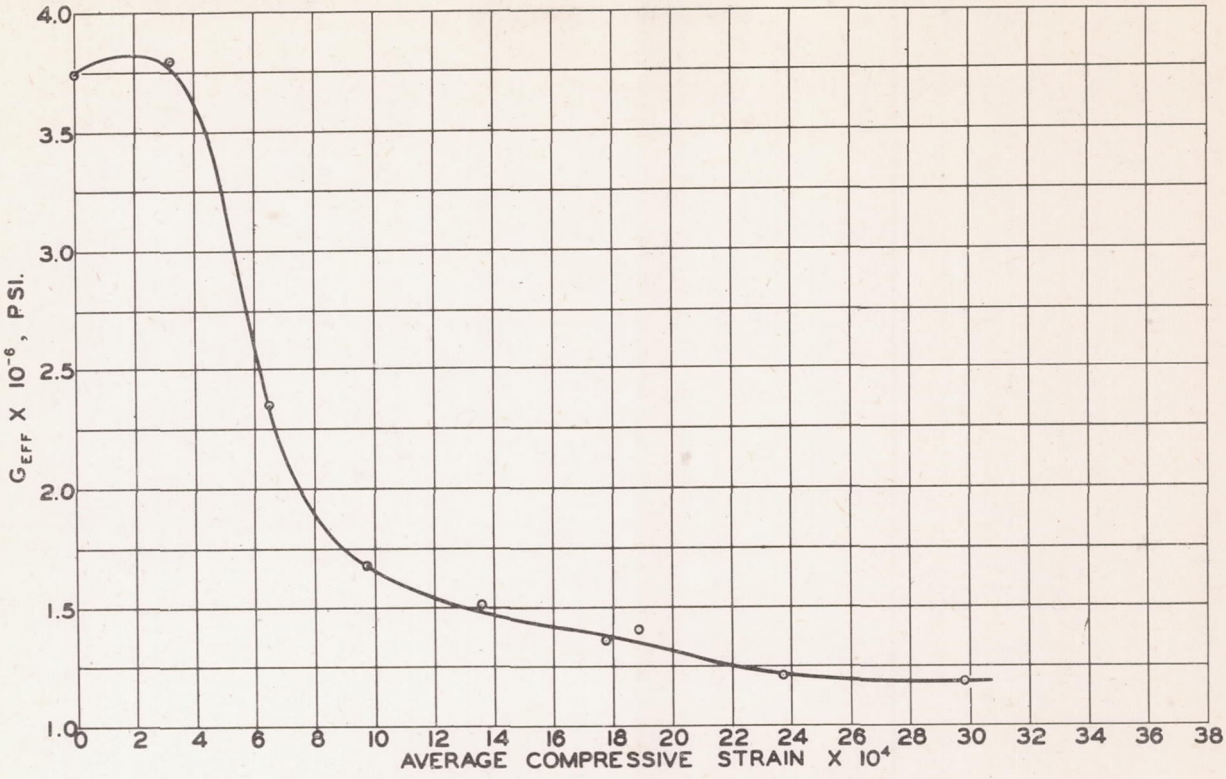


FIG. 19.- VARIATION OF EFFECTIVE SHEAR MODULUS G_{EFF} WITH AVERAGE COMPRESSIVE STRAIN.

CYLINDER 31

DIAMETER D = 16" 12 STRINGERS RING SPACING 4.5"
SHEET THICKNESS t = 0.012" SHEET MATERIAL 24 ST ALCLAD
RINGS NOT RIVETED TO SHEET

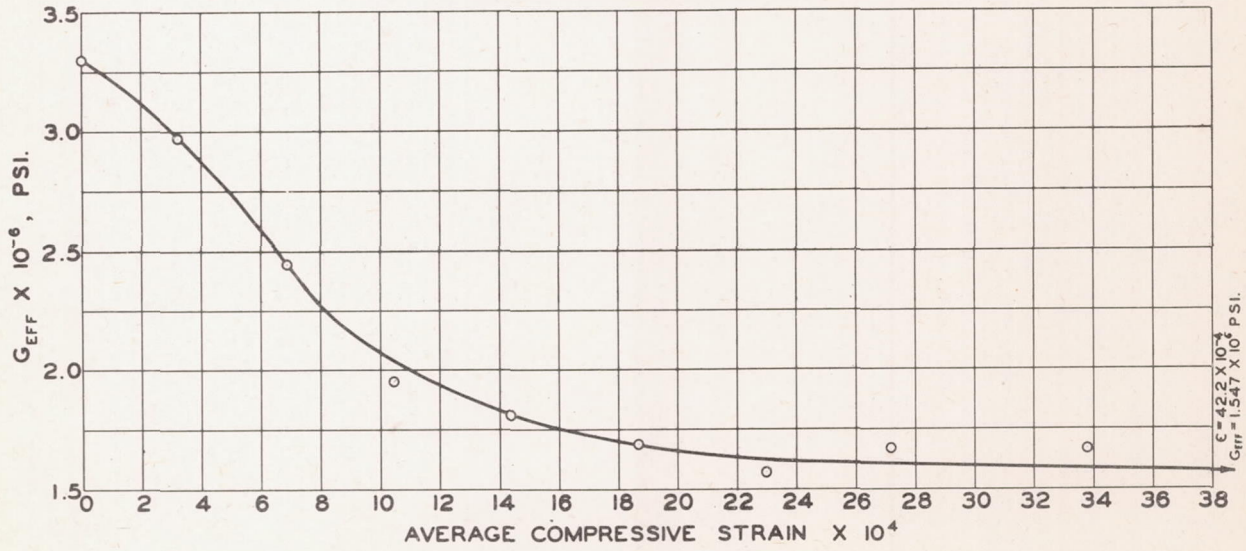


FIG. 20.- VARIATION OF EFFECTIVE SHEAR MODULUS G_{EFF} WITH AVERAGE COMPRESSIVE STRAIN.

CYLINDER 32

DIAMETER D = 16" 12 STRINGERS RING SPACING 2.57"
SHEET THICKNESS t = 0.012" SHEET MATERIAL 24 ST ALCLAD

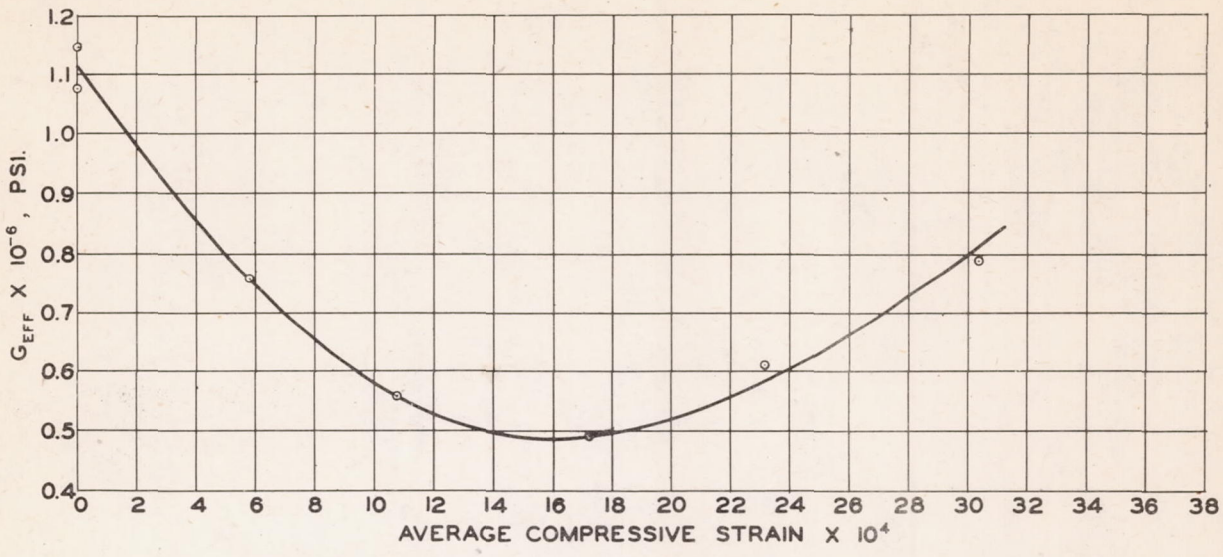
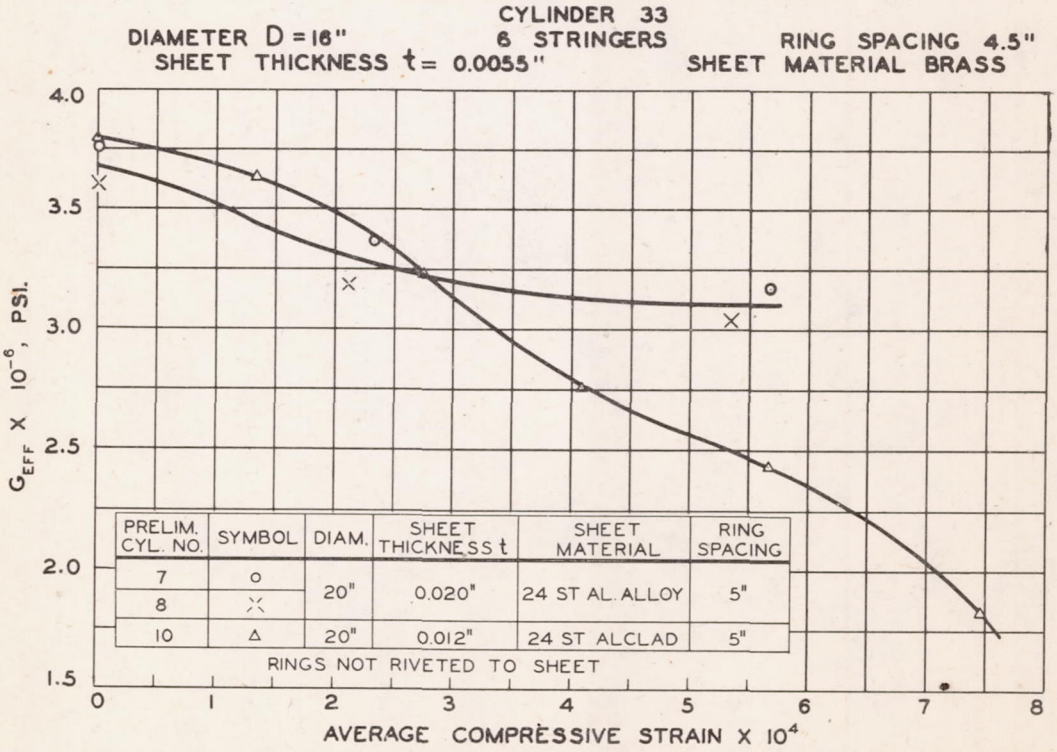


FIG. 21.- VARIATION OF EFFECTIVE SHEAR MODULUS G_{EFF} WITH AVERAGE COMPRESSIVE STRAIN.



PRELIM. CYL. NO.	SYMBOL	DIAM.	SHEET THICKNESS t	SHEET MATERIAL	RING SPACING
7	o	20"	0.020"	24 ST AL. ALLOY	5"
8	×				
10	△	20"	0.012"	24 ST ALCLAD	5"

FIG. 22.- VARIATION OF EFFECTIVE SHEAR MODULUS G_{EFF} WITH AVERAGE COMPRESSIVE STRAIN.
PRELIMINARY SERIES CYLINDERS 7, 8, 10.

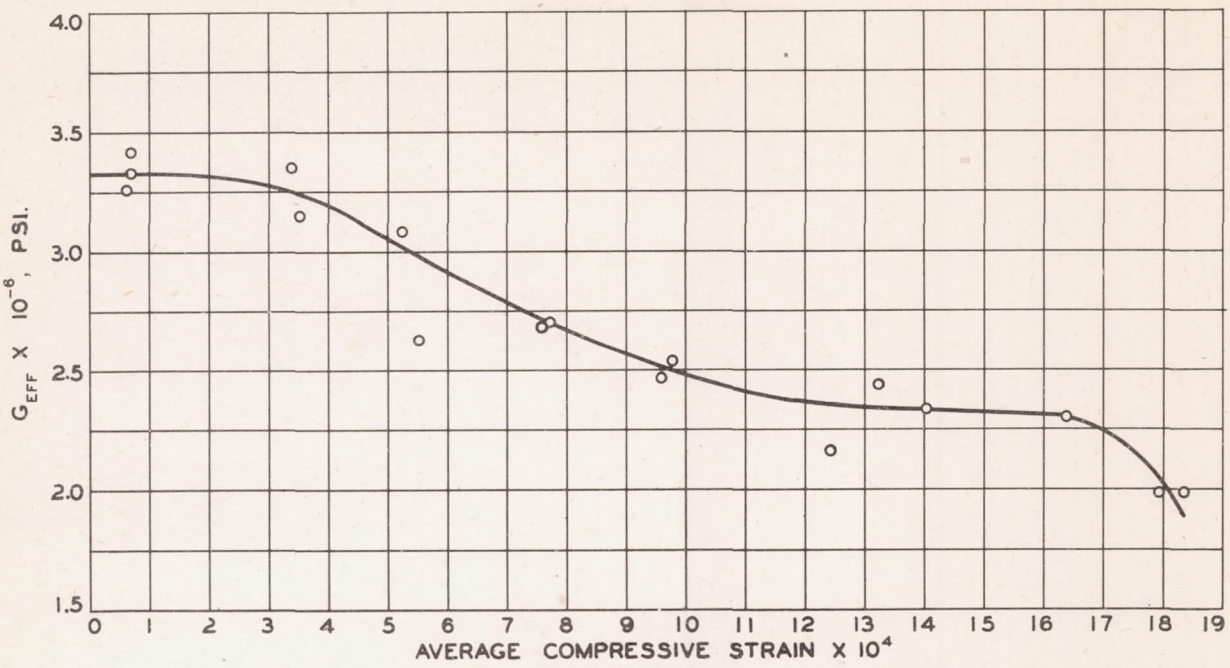


FIG. 23.- VARIATION OF EFFECTIVE SHEAR MODULUS G_{EFF} WITH AVERAGE COMPRESSIVE STRAIN.

PRELIMINARY SERIES CYLINDER 15

DIAMETER D = 16" SHEET THICKNESS t = 0.012" SHEET MATERIAL 24 ST ALCLAD
16 STRINGERS RING SPACING 5" RINGS NOT RIVETED TO SHEET

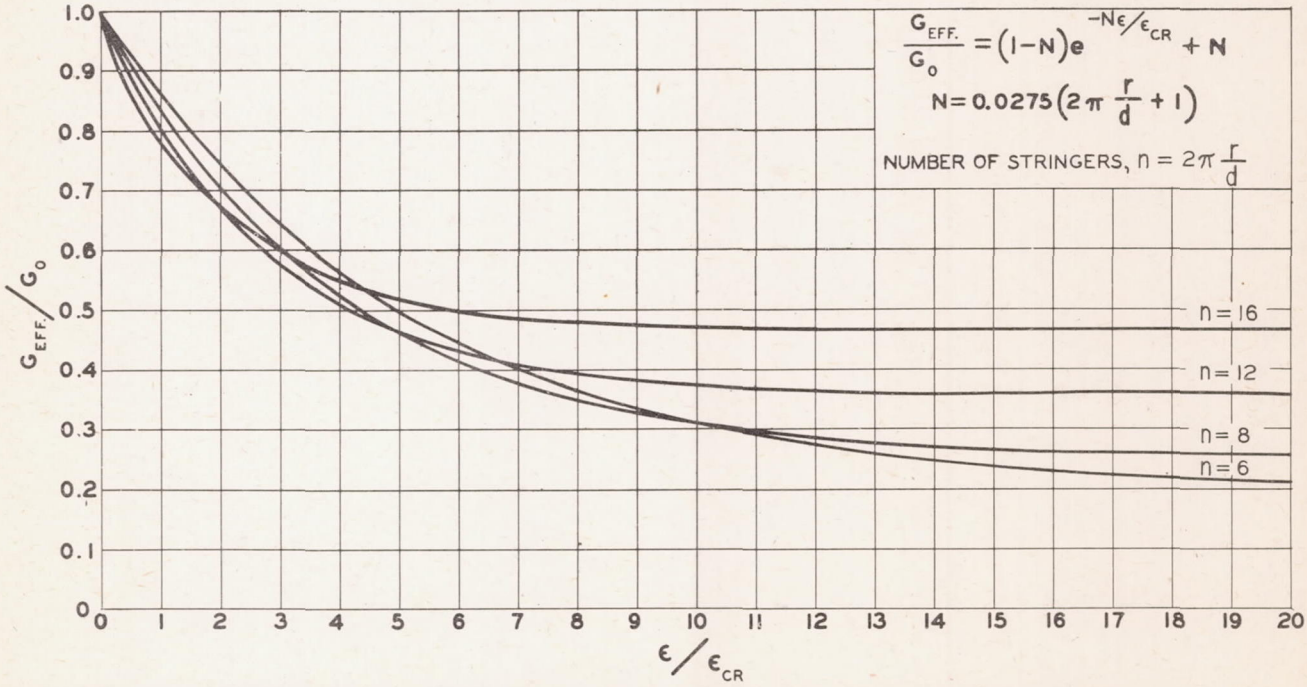


FIG. 26.- NON-DIMENSIONAL SHEAR RIGIDITY CURVES

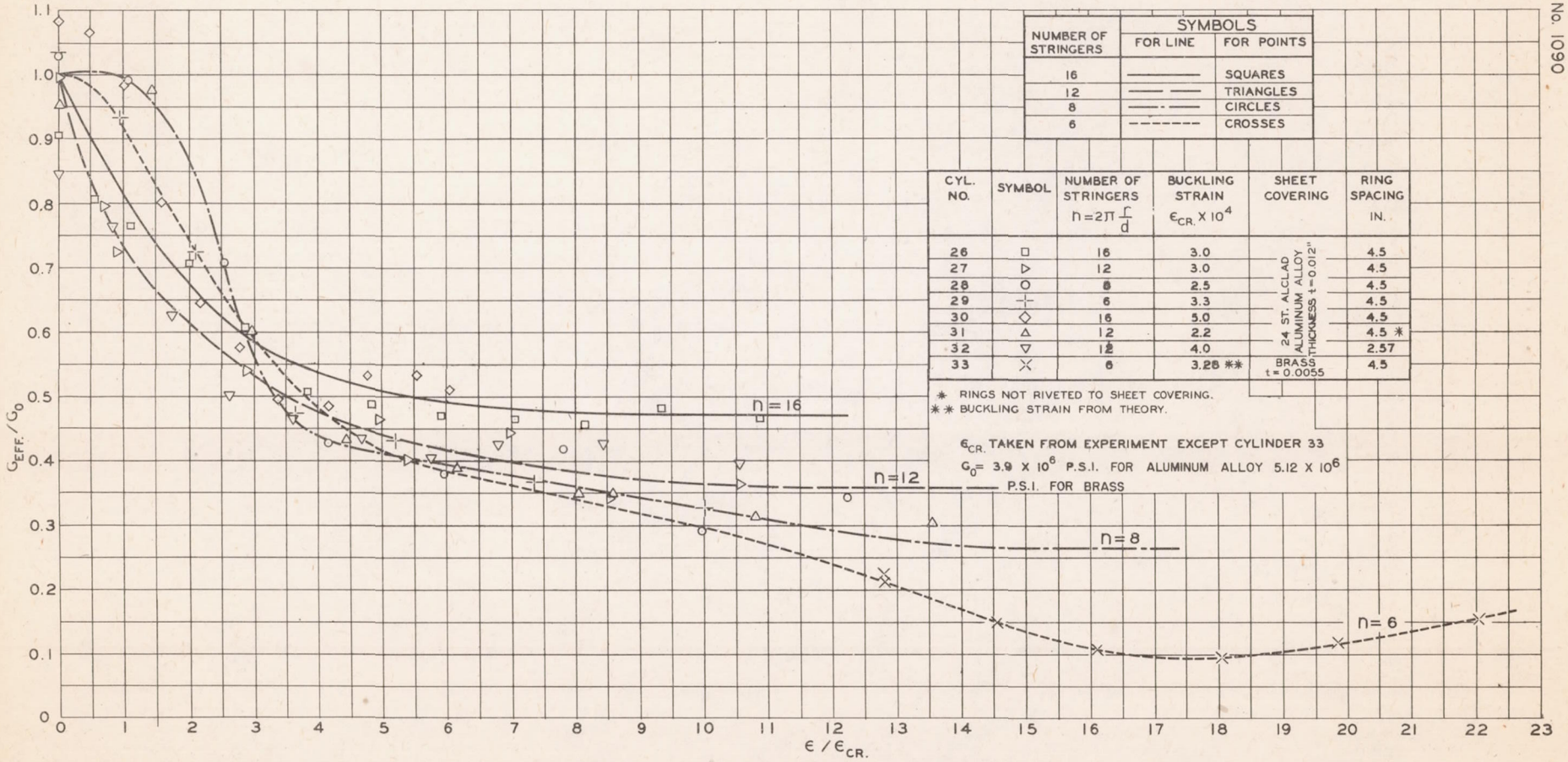


FIG. 24.- EXPERIMENTAL NON-DIMENSIONAL SHEAR RIGIDITY CURVES.

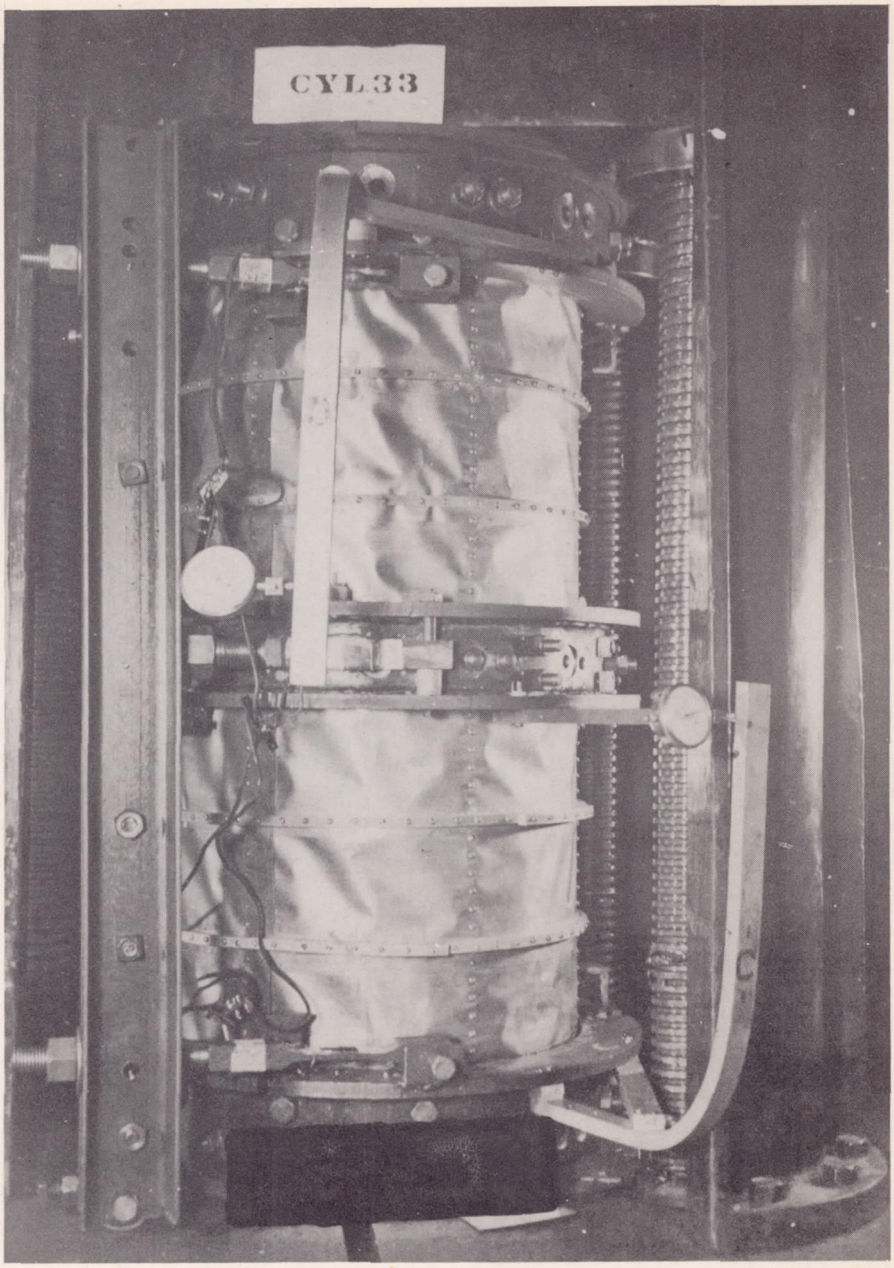


Figure 25.- Cylinder 33 under load. P = 23,000 lb.

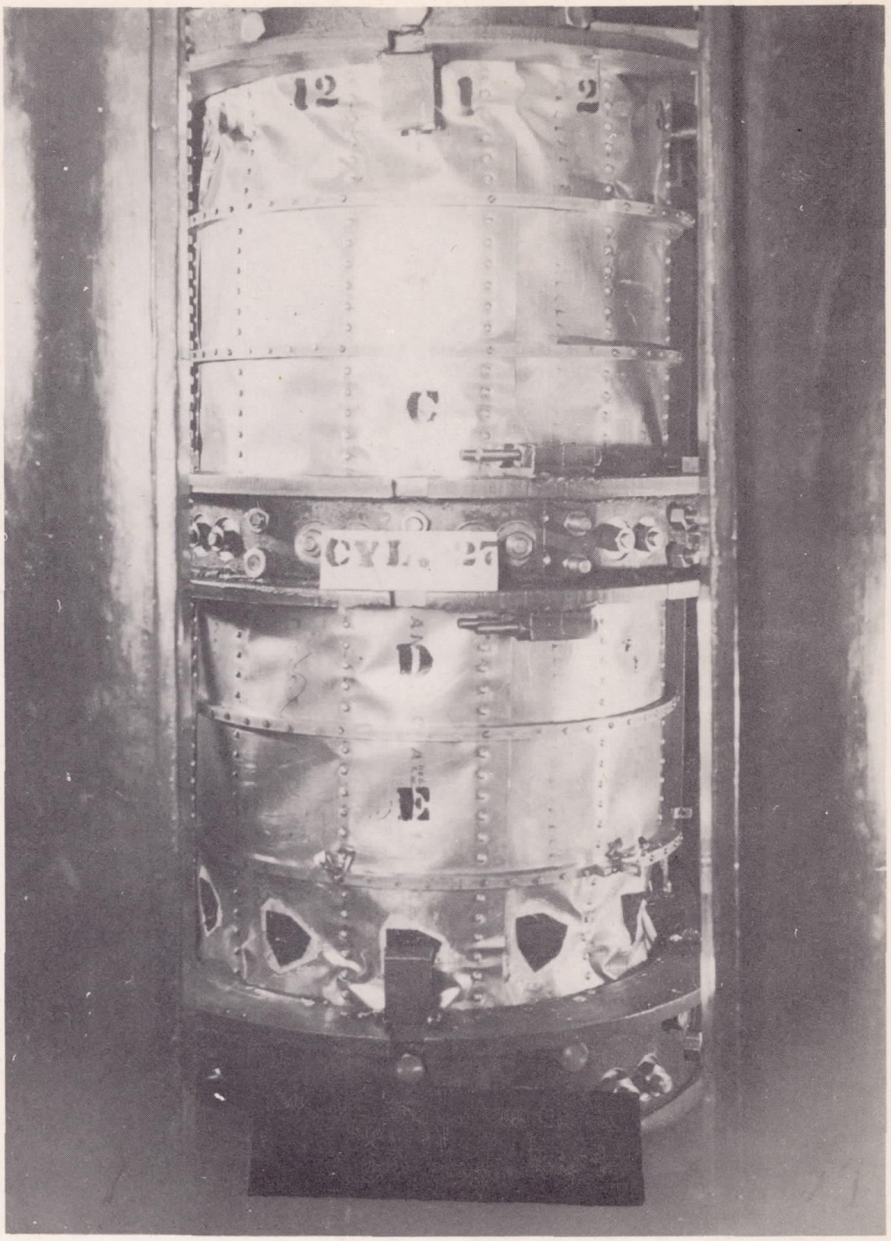


Figure 27.- Cylinder 27 after failure.

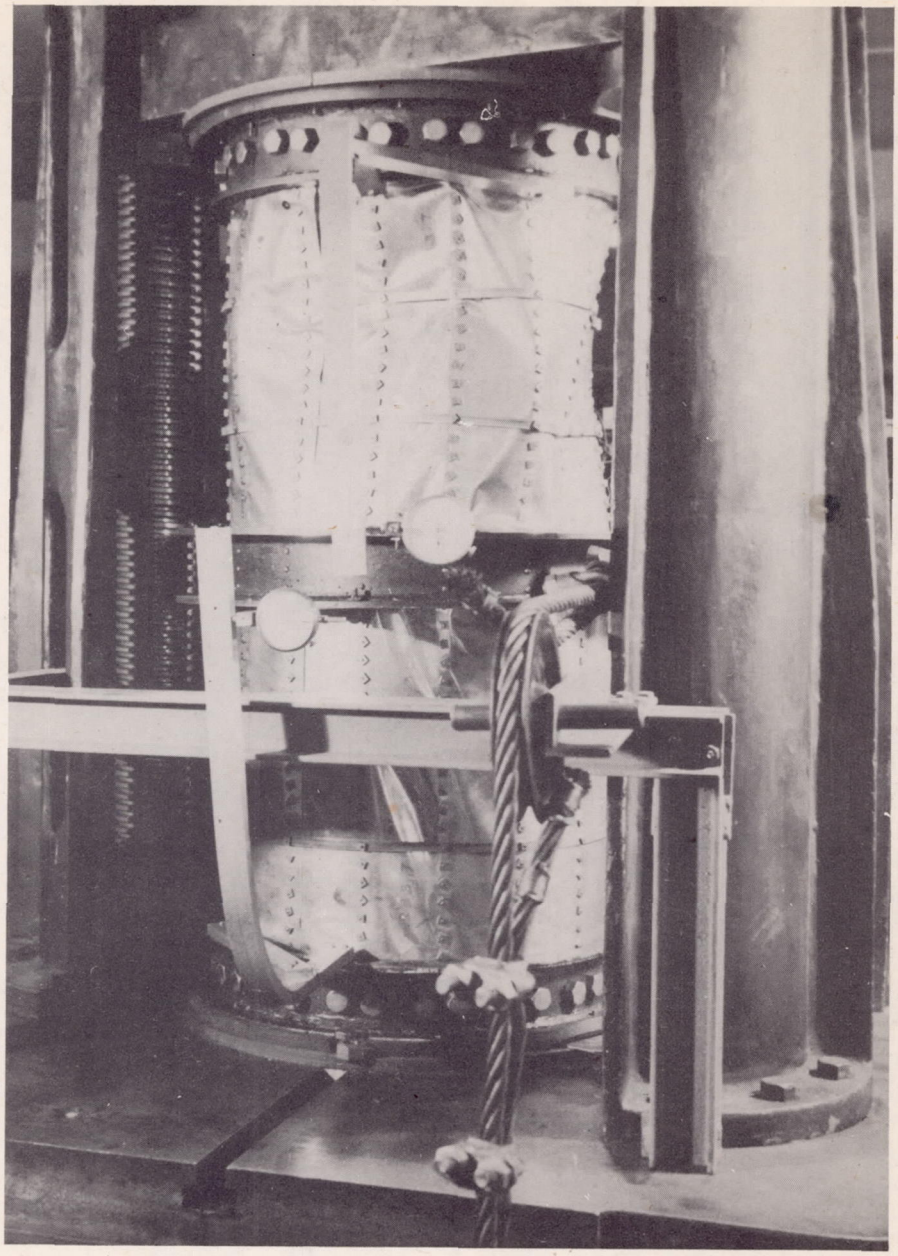


Figure 28.- Cylinder 15 after failure.